FGF and BMP pathway genes are expressed in segmentally iterated domains during segmentation of germ layers in a tardigrade

Kira L. Heikes[1,2], Lillian D. Papell[1], Noemi Gavino-Lopez[1], and Bob Goldstein[1,2,3,*]

[1] Biology Department, University of North Carolina at Chapel Hill, Chapel Hill, NC, USA
[2] Curriculum in Genetics and Molecular Biology, University of North Carolina at Chapel Hill, Chapel Hill, NC, USA
[3] Lineberger Comprehensive Cancer Center, University of North Carolina at Chapel Hill, Chapel Hill, NC, USA
[*] Corresponding author: Department of Biology, University of North Carolina at Chapel Hill, 616 Fordham Hall, Campus Box 3280, Chapel Hill, NC 27599-3280
E-mail: bobg@unc.edu

Keywords: Tardigrades, BMP, FGF, Segmentation, Mesoderm

Bullet Points:

- Double mRNA detection in tardigrades revealed expression patterns of FGF and BMP pathway genes
- *fgf8* was detected primarily in ectoderm but absent from internal germ layers, and *fgfrl1* was detected in all layers and enriched in internal layers
- *dpp* was detected more dorsally than *sog* in lateral ectoderm
- *fgf8* and *dpp* gene expression exhibit different segmentally iterated domains in ectoderm
- Results suggest specific hypotheses for roles for FGF signaling and BMP signaling in tardigrade development

Abstract

Background:

A small number of signaling pathways regulates development in most animals, yet we do not know where these pathways are deployed in embryos of many animal phyla. Filling such gaps can contribute to understanding how diverse body shapes arise from differential deployment of conserved signaling pathways. Here, we examined where conserved pathways are deployed in tardigrades, a panarthropod phylum with miniaturized, segmented bodies.

Results:

We used *in situ* mRNA detection in the tardigrade *Hypsibius exemplaris* to reveal expression patterns of FGF and BMP signaling pathway components during body segmentation and early mesoderm development. Among the patterns examined, we found an FGF ligand and receptor expressed near each other in segmentally iterated regions of ectoderm and endomesoderm, respectively. We also found a BMP ligand and antagonist expressed in dorsoventrally-restricted patterns in the lateral ectoderm.

Conclusions:

The detected patterns suggested specific hypotheses for further research: possible FGF signaling between ectoderm and endomesoderm, and possible roles of BMP signaling in dorsal-ventral patterning of lateral ectoderm. We compared our results with published expression patterns for FGF and BMP pathways across panarthropods, to contribute to previous hypotheses for how the development of segments and mesoderm may have evolved in the emergence of this clade of diversly-shaped animals.

Introduction

Embryonic development relies on precise temporal and spatial patterning to form specific body shapes. Organisms come in many unique shapes, as the result of unique developmental trajectories, yet each trajectory relies on widely conserved cell signaling pathways. Among animals, these include the FGF, BMP, EGF, TGF-β, Wnt, Hedgehog, Hippo, and Notch signaling pathways (Pires-daSilva and Sommer, 2003). There is a breadth of knowledge about how cell signaling refines developmental patterns in common model organisms (Pires-daSilva and Sommer, 2003). Much less is understood about how cell signaling facilitates the formation of other body forms. Such gaps limit our understanding of what is possible in the toolkit to build an embryo.

Addressing such gaps is possible with comparisons across developmental programs, particularly among closely related animals with differently shaped embryonic body plans. Ecdysozoa is a group of diversly shaped animals that includes the well-studied model systems *C. elegans* and *D. melanogaster*, as well as many emerging model systems (Giribet and Edgecombe, 2017; Telford et al., 2008). Panarthropoda is a subset of Ecdysozoa, those with segmented bodies, consisting of the arthropods (including *D. melanogaster*), onychophorans, and tardigrades (Howard et al., 2022; Telford et al., 2008). The repeating body segments of panarthropod animals are defined by a mostly homologous order of Hox gene expression in embryonic stages, yet panarthropods exhibit widely diverse adult structures (Akam, 1995; Franke and Mayer, 2014; Hughes and Kaufman, 2002; Janssen, 2017; Janssen et al., 2014; Peel et al., 2005; Smith et al., 2023, 2016; Smith and Goldstein, 2017). Such embryonic homology affords a powerful platform for building hypotheses of how different developmental trajectories transform these seemingly homologous segments into very different shapes.

Positional information from cell signaling contributes to regulating differentiation of the germ layers and specifying the location, size, and morphology of tissue folds, organs, and appendages during development. Therefore, we can learn more about how homologous body segments are refined into a variety of structures by detecting where conserved pathways are deployed in body segments of species from across panarthropoda. Tardigrades comprise an entire phylum of panarthropod animals whose

development is little studied compared to its arthropod relatives. We sought to uncover where conserved signaling pathways are deployed in a tardigrade species during and immediately following the emergence of body segments in embryos, to inform comparisons made across panarthropods.

The tardigrade body plan consists of a head with two eyes and four leg-bearing trunk segments and is uniquely miniaturized among panarthropods, with tardigrade body regions likely homologous to just the head and very posterior of arthropod and onychophoran bodies (Gross et al., 2019; Schill, 2018; Smith et al., 2016; Smith and Goldstein, 2017). One species of tardigrade, *H. exemplaris*, is an emerging model system, with established methods for *in situ* hybridization to visualize gene expression patterns (Gabriel et al., 2007; Goldstein, 2018; Goldstein and Blaxter, 2002; Heikes et al., 2023; Smith, 2018). Harnessing the spatial and temporal information provided from *in situ* hybridization, previous studies have shed light on mechanisms that may explain how the tardigrade's segmented body was miniaturized from the panarthropod ancestor, by comparing expression patterns between tardigrades, onychophorans, and arthropods. These proposed mechanisms include 1) loss of an entire body region and associated hox genes, 2) loss of an intermediate leg region and associated leg gap gene with broader expression of remaining leg gap genes, and 3) loss of several Wnt ligand genes and a lack of segmentally iterated expression of the remaining Wnt ligands (Chavarria et al., 2021; Game and Smith, 2020; Smith et al., 2023, 2016). We took an approach also relying on *in situ* hybridization to reveal where members of conserved signaling pathways are deployed during early stages of endomesodermal and ectodermal segmentation, which reflect the first anatomical evidence of body segments in *H. exemplaris* embryos.

The Fibroblast Growth Factor (FGF) and Bone Morphogenetic Protein (BMP) conserved pathways are frequently deployed in refinement of endomesoderm and ectoderm across animal embryos, including members of Panarthropoda (Andrikou and Hejnol, 2021; Beermann and Schröder, 2008; Donoughe et al., 2014; Ewen-Campen et al., 2013; Fan et al., 2018; Green et al., 2013; Hamaratoglu et al., 2014; Hogvall et al., 2018; Huang and Stern, 2005; Janssen et al., 2015; Kainz, 2009; Kimelman and Kirschner, 1987; Matus et al., 2007; Muha and Müller, 2013; Nakamura and Extavour,

2016; Pechmann et al., 2017; Sharma et al., 2015; Stathopoulos et al., 2004; Suzuki et al., 1994; Treffkorn and Mayer, 2013; Van Der Zee et al., 2006; Wijesena et al., 2017; Winnier et al., 1995). BMP and FGF signaling also integrate with and feed back on one another during mesoderm development in animals, including panarthropods studied thus far (Kimelman and Kirschner, 1987; Luo, 2017; Row et al., 2018; Stathopoulos et al., 2004; Wang et al., 2023). Therefore, examining expression patterns of genes from both pathways may shed light on spatiotemporal refinement of ectoderm and mesoderm in the body segments of *H. exemplaris* embryos.

Using double fluorescence *in situ* hybridization (FISH) to simultaneously detect expression patterns of two genes at a time in embryos of the tardigrade *H. exemplaris*, we revealed the spatiotemporal expression of FGF and BMP pathway genes during the processes of endomesodermal segmentation and subsequent ectodermal segmentation. Based on these observed patterns and known roles in other animals, we present hypotheses about where genes may have been expressed in the ancestral panarthropods and about the potential roles of FGF and BMP signaling in refining tardigrade body shape during segmentation and mesoderm development, which will be testable upon expansion of genetic tools for use in tardigrade embryos.

Results and Discussion

Identification of conserved signaling pathway genes in *H. exemplaris*

We identified putative homologs for genes encoding members of the FGF and BMP signaling pathways in *H. exemplaris*. We searched for upstream pathway components and putative target genes, as these are most likely to be differentially expressed. We identified all likely homologs in published *H. exemplaris* transcriptomes (Levin et al., 2016; Yoshida et al., 2017) by NCBI's tBLASTn search, using *D. melanogaster* protein sequences as queries (Kent et al., 2002) and validating by reciprocal BLASTp against the *D. melanogaster* protein database to confirm that identified homologs returned the original query (Altschul et al., 1990; Gerts et al., 2006; Sayers et al., 2022). We analyzed top hits further with protein domain database tools to confirm protein structures matched those of the queries (Letunic et al., 2021; Letunic and Bork, 2018). We sought further support of gene homology for top hits of query protein sequences

through maximum likelihood phylogenetic reconstruction of likely sequence evolution among homologs and orthologs from other ecdysozoan and non-ecdysozoan species, with branch support from 500 bootstraps [details in Experimental Procedures] (Kumar et al., 2018). Support varied from gene to gene, and we tentatively assigned gene names based on the support we found and the BLAST results, domain analyses, and alignments; below each phylogenetic tree, we show an alignment of the sequences used to build the trees, capturing a subset of the species represented in each tree [Supp. Figs. 2-9]. We consulted a published staged transcriptome through *H. exemplaris* development to aid in prioritizing genes for mRNA detection by FISH at our developmental stages of interest – endomesodermal and ectodermal segmentation (Levin et al., 2016).

For the FGF pathway in published *H. exemplaris* transcriptomes, we identified one FGF ligand homolog: *fgf8* (Supp. Fig. 1) and two homologs of FGF receptors: *fgfrl1* and *fgfrl2* (FGF receptor-like 1 and 2, respectively, Supp. Fig. 2). Expression levels in the published staged transcriptome suggested to us that *fgfrl1* is expressed at high enough levels for detection by fluorescence *in situ* hybridization (FISH), but *fgfrl2* is very weakly expressed (Levin et al., 2016). Our preliminary staining by chromogenic *in situ* hybridization also aligned with this prediction, as we detected low to no signal of *fgfrl2* during segmentation stages (data not shown). We concluded that *fgfrl1* is likely to be relevant during these stages of embryonic development in *H. exemplaris* and moved forward with this gene to identify cells likely to be receptive to FGF signaling. The *H. exemplaris* homolog of *fgf8* was not represented in the staged transcriptome, so we could not consult it for expected expression levels. We also identified one homolog of the mesodermal transcription factor *snail* in hopes of using it as a marker of embryonic mesoderm and potential FGF responsive cells, since FGF is known to regulate mesoderm development (Supp. Fig. 3). This *snail* homolog was weakly expressed in the staged transcriptome (Levin et al., 2016).

For the BMP pathway in published *H. exemplaris* transcriptomes, we found one homolog each of the BMP2/4-type ligand *decapentaplegic* (*dpp*), the BMP5/6/7/8-type ligand *glass bottom boat* (*gbb*) (Supp. Fig. 4), the extracellular BMP antagonist *short gastrulation* (*sog*) (Supp. Fig. 5), the Type 1 and Type 2 BMP receptors (Supp. Fig. 6)

thickveins and *punt*, the Type 1 BMP receptors *saxophone* and *baboon*, and the Sog-cleaving protease *tolloid* (Supp. Fig. 7). We also identified one homolog each of known downstream transcriptional targets of BMP signaling in arthropods as potential markers of BMP responsive cells: *dorsocross1* (*doc1*) and *eyes absent* (*eya*) (Supp. Fig. 8 and Supp. Fig. 9) (Dominguez et al., 2016). FGF signaling has also been found to target *eya* expression (Ahrens and Schlosser, 2005). All of these identified homologs were highly expressed between elongation and segmentation stages in the published staged transcriptome (Levin et al., 2016). Another known target of BMP signaling in arthropods, *c15* (*clawless*), was cloned in a previous publication, which reported its expression domains at post-segmentation stages in developing limbs (Mapalo et al., 2024).

We refer to these genes by their likely homologs' names moving forward. Using FISH, we detected where each of these upstream signaling pathway genes and putative target genes is expressed during segmentation of *H. exemplaris* embryos. Although mRNA distributions are affected by mRNA synthesis, localization, persistence, and depletion, we refer to the presence of mRNA, detected by FISH, as gene expression for simplicity. A summary of the relevant embryonic stages examined is presented in Fig. 1. In the sections that follow, we present detected expression of components of FGF signaling first and of BMP signaling second.

By ectodermal segmentation, FGF ligand *fgf8* is expressed in segmentally iterated patches of ectodermal cells and FGF receptor *fgfrl1* is enriched in underlying endomesodermal pouches.

To reveal likely FGF-sending and FGF-receiving cells, we simultaneously detected where *fgf8* and *fgfrl1* are expressed at 24 hours post laying (hpl) when ectodermal and endomesodermal segments are both anatomically apparent. Among arthropods studied thus far, gene homologs of the FGF ligand *fgf8* are expressed in or near the developing foregut, in a region of the head segment that defines the midbrain-hindbrain boundary, and in a posterior growth zone in species that undergo posterior growth, which then persists in the posterior of body segments as they form from the growth zone (Beermann and Schröder, 2008; Kainz, 2009; Muha and Müller, 2013; Stepanik et al., 2020). The fruit fly *D. melanogaster* does not undergo posterior growth but still exhibits

segmental expression of its *fgf8* homologs in ectoderm (Stepanik et al., 2020). Current evidence suggests that onychophorans do not undergo posterior growth, and FGF signaling has yet to be studied in an onychophoran system (Hogvall et al., 2014; Mayer et al., 2010). Tardigrades also do not undergo posterior growth (Hejnol and Schnabel, 2005; Smith et al., 2016; Smith and Goldstein, 2017). We found that *fgf8* was expressed in a segmentally iterated pattern in the ectoderm – in patches of lateral ectodermal cells in the posterior of each trunk segment on both the left and right sides of embryos (Fig. 2 and Video 1). A patch of *fgf8* expression was detected laterally near the middle of the head segment in ectoderm, potentially contributing to regional patterning of the brain, which may still occur at the level of cell fates within the unipartite brain structure of tardigrades (Smith et al., 2018). Another patch of *fgf8* expression was detected in a small set of cells at the posterior of the head segment in ectoderm and endomesoderm, likely where the esophagus develops from foregut (Fig. 2). While *fgf8* was expressed in a segmentally repeating pattern in the ectoderm, *fgfrl1* was expressed broadly in the embryo and enriched in the endomesodermal pouches found within each of the four trunk segments, in the developing foregut in the head segment, and to a lesser extent in the ectoderm (Fig. 2 and Video 2). This is consistent with a possibility that all mesoderm is receptive to FGF8 signal, and that FGF8 might pattern the underlying *fgfrl1*-expressing mesoderm in addition to *fgfrl1*-expressing ectoderm. Segmentally iterated posterior patches of *fgf8* may be ancestral to panarthropod species; however, addressing this demands data from a larger sampling of panarthropods, especially onychophorans.

We next wondered how early these patches of *fgf8* emerge relative to the anatomical appearance of body segments, since by 24 hpl, body segments are 3 hours old (Fig. 1 A).

Segmentally iterated *fgf8* expression appears prior to ectodermal segmentation and near the time when endomesodermal pouches form.

To determine if segmentally iterated *fgf8* expression preceded, arose concomitantly with, or followed body segmentation, we detected expression at earlier stages – at late elongation (~18 and 19 hpl) before segments are apparent, at endomesodermal pouch

formation (~20 hpl) when endomesoderm begins to appear segmentally divided, and at early ectodermal segmentation (~21-22 hpl) when ectoderm begins to appear segmentally divided (Fig. 1 A). These stages correspond to stages 11-13 from previous publications (Chavarria et al., 2021; Gabriel et al., 2007). Between 18 hpl and 22 hpl, *fgfrl1* was enriched in endomesodermal cells, and this pattern did not change dramatically. In contrast, the number of ectodermal domains expressing *fgf8* increased over time in this period. At elongation stages, there were fewer, broad patches of ectodermal *fgf8* expression than at later stages (Fig. 3 A-A''' and Supp. Fig. 10). Additionally, the patches of cells expressing *fgf8* appeared first in the anterior half of the embryo at elongation stages and only later when endomesoderm was segmented did they line the embryo from anterior to posterior. Following or concomitant with ectodermal segmentation (~21-22 hpl), ectodermal patches of *fgf8* expression began to resemble what we saw at 24 hpl, i.e. segmentally iterated, in lateral pairs in the posterior of each trunk segment and in the middle of the head segment, in addition to expression in a small group of cells in the posterior of the head segment (Fig. 3 C-C''' and D-D'''). Ectodermal segmentation is evident by the presence of furrows in the ectoderm at the approximate boundaries between body segments (Fig. 1) (Chavarria et al., 2021; Gabriel, 2007; Gabriel et al., 2007; Gabriel and Goldstein, 2007). At 20 hpl, when endomesodermal pouches have formed but ectodermal segmentation has not occurred, patches of *fgf8* expression were present in the lateral ectoderm on each side of the embryo (Fig. 3 B-B'''). This expression pattern reveals that enrichment of *fgf8* in the ectoderm of each segment precedes apparent anatomical segmentation of ectoderm and either follows or occurs concomitantly with segmentation of endomesoderm.

FGF plays a role in posterior segment polarity in deuterostomes, along with Wnt. Thus far, evidence in ecdysozoans, a protostome superclade, only suggests a role of Wnt in posterior segment polarity, not FGF (Angelini and Kaufman, 2005; McGregor et al., 2008; Miyawaki et al., 2004). FGF does have a functional role in segment number in the beetle *Tribolium castaneum* and in segment size in the cricket *Gryllus bimaculatus*, but these roles are difficult to untangle from FGF's function in body extension in these arthropods that undergo posterior growth (Kainz, 2009; Sharma et al., 2013). Expression of *fgf8* in segment posteriors across arthropods and in a tardigrade suggest

this may be an unidentified role for FGF in panarthropods, but ruling this out confidently demands data from a larger representation of panarthropod species. If FGF8 is a segment polarity cue in tardigrades, then endomesodermal pouch formation might follow *fgf8* mRNA patch formation. We were unable to resolve the order in which these events occur, as we never saw an embryo with patches of *fgf8* mRNA but an unsegmented endomesoderm or vice versa. This would require a study using a live fluorescent reporter of *fgf8* mRNA, such as the MS2-MCP system, and DIC imaging of embryo morphology (Bertrand et al., 1998; Garcia et al., 2013; Lucas et al., 2013; Wu et al., 2012). Related to this, another study found by antibody staining that Engrailed protein, which is also expressed in segment posteriors, appears only after formation of endomesodermal pouches (Gabriel and Goldstein, 2007). Therefore, FGF8 might be an instructive cue for Engrailed expression, further reinforcing the posterior boundary of segments.

The patches of *fgf8* expression also appeared to change in orientation relative to the axes of the embryo. Upon ectodermal segmentation, the patches were positioned in cells in the posterior of each segment and had elongated forms that were aligned perpendicularly to the anterior-posterior axis (Fig. 2 and Fig. 3 C and D). Prior to ectodermal segmentation, the patches were elongated parallel to the anterior-posterior axis, along the segments (Fig. 3 B). Therefore, the pattern of *fgf8* is dynamic, or the *fgf8*-expressing cells move or change shape, during ectodermal segmentation of the embryo. FGF8 often serves as a guidance cue for mesodermal migration, and if this is the case in *H. exemplaris*, then this change in orientation of the *fgf8* patches may be an important directional cue (DeVore et al., 1995; Gryzik and Muller, 2004; Kadam et al., 2012; Klingseisen et al., 2009; Röttinger et al., 2008; Sharma et al., 2015). Alternatively or in addition, the underlying mesoderm, as it migrates, may feed back on *fgf8* to influence the direction of the patches and the formation of ectodermal segments, which appears to occur concomitantly with the re-orienting of *fgf8* patches, though determining this also requires the use of live imaging tools.

The mesodermal transcription factor *snail* is expressed in non-mesodermal cells.

To determine more precisely which cells in endomesodermal pouches contribute to the mesoderm, we detected expression for the ectodermal transcriptional repressor *snail*, which historically serves as a marker of mesodermal fate in animal embryos, together with the pro-mesodermal transcription factor *twist* (Leptin, 1991). However, *snail* was expressed throughout the embryo, in both ectodermal and endomesodermal layers of cells at both elongation and ectodermal segmentation stages (Fig. 4). Expression of *snail* appeared to become more enriched in the internal endomesodermal cells by 24 hpl but was still present in ectodermal cells (Fig. 4 A-D). Therefore, *snail* expression may not be a reliable marker of mesodermal fate at this stage in development. By double FISH, *snail* was expressed in cells that expressed *fgfrl1* (Fig. 4 A-A''' and B-B''') and in cells that expressed *fgf8* (Fig. 4 C-C''' and D-D'''). Given this overlap, this expression pattern suggests that *snail* is expressed in both FGF sending and FGF receiving cells.

This expression pattern of *snail* was surprising, given that in other systems, Snail serves as a marker and promoter of mesoderm fate through inhibition of non-mesodermal genes (Alberga et al., 1991; Cano et al., 2000; Chopra and Levine, 2009; Simpson, 1983). Although it does not appear to be a reliable marker of mesodermal fate at these stages in *H. exemplaris* development, the expression pattern of *snail* is potentially reflective of aspects of mesodermal development in this system. It is possible that either mesoderm migrates from many starting points in development, including the ectoderm layer, or that many nonmesodermal cells express *snail* and only later in development is *snail* restricted to mesoderm. It is also possible that *snail* instead marks neuroectoderm as it internalizes from the surface of the embryo, as *snail* marks neuroectoderm in many panarthropods and other animal systems studied (Erives et al., 1998; Hannibal et al., 2012; Hemavathy et al., 1997; York et al., 2019).

Based on all of our results examining expression of FGF pathway genes, we conclude that the ligand-encoding gene *fgf8* is expressed primarily in lateral ectoderm in the posterior of each body segment, as well as in the head, and the receptor-encoding gene *fgfrl1* is expressed broadly and enriched in endomesoderm, including in pouches underlying each ectodermal *fgf8*-expressing patch of cells.

BMP ligand *dpp* and antagonist *sog* are expressed in lateral ectoderm, and *dpp* is expressed more dorsally than *sog*.

To determine where components of the BMP signaling pathway are expressed at an ectodermal segmentation stage (24 hpl), we detected expression of BMP receptors *tkv* and *punt* (which frequently heterodimerize and bind *dpp*), BMP ligands *dpp* and *gbb*, BMP antagonist *sog*, and Sog-cleaving protease *tld* (Mullins, 1998; Nunes da Fonseca et al., 2010; Ramel and Hill, 2012). By single FISH, receptors *tkv* and *punt* were ubiquitously expressed across the embryo, consistent with a possibility that all cells may be receptive to BMP signaling (Supp. Fig. 11). However, the precise pattern of cells receptive to BMP signaling via Gbb and/or Dpp may be further refined by the expression patterns of other BMP receptor genes, such as *saxophone* and *baboon*. BMP5/7/8-type ligand Gbb regulates development of the germ cells in the arthropod *G. bimaculatus*, as well as in vertebrate systems, but so far BMP signaling has not been implicated in germ cell development in other panarthropods (Donoughe et al., 2014; Lawson et al., 1999; Lochab and Extavour, 2017). In *H. exemplaris*, the ligand *gbb* was ubiquitously expressed throughout most of the embryo (Supp. Fig. 12). However, *gbb* expression appeared to be absent from the cells previously defined as the primordial germ cells (Heikes et al., 2023) but present in somatic cells surrounding the primordial germ cells (Supp. Fig. 12), whereas receptors *tkv* and *punt* were expressed in the primordial germ cells (Supp. Fig. 11). This expression pattern is consistent with a possibility that signaling by Gbb might regulate primordial germ cell development in this tardigrade species.

In arthropods and onychophorans, BMP2/4-type ligand gene *dpp* is expressed along the trunk near trunk ganglia, near the developing mouth, and in the anlage of limbs, and is known to regulate embryo dorsal-ventral patterning, mesoderm differentiation, nervous system development, and appendage patterning (Donoughe et al., 2014; Morisato and Anderson, 1995; Nakayama et al., 2000; Ramel and Hill, 2012; Winnier et al., 1995). By double FISH, the ligand *dpp* and the antagonist *sog* were expressed in ventro-lateral ectoderm (Fig. 5 and Video 3). Neither gene was appreciably expressed in the most dorsal regions of the embryo (Fig. 5 C and Video 4). *dpp* was expressed in

more dorsal regions of lateral surfaces than *sog* (Fig. 5 C). This lateral enrichment of *dpp* and *sog* is consistent with a possible role for Dpp in dorsal-ventral patterning of lateral ectoderm, perhaps by elaborating fates along the dorsal-ventral axis, rather than symmetry breaking, as symmetry breaking in the dorsal-ventral axis has already occurred by this stage of *H. exemplaris* development. Alternatively or in addition, this expression pattern is consistent with a potential role for Dpp in regulating development of the neural trunk ganglia that run in parallel rows from anterior to posterior along the animal's ventral surface.

At the anterior-most tip of the head where the mouth likely develops, *sog* was expressed in bands on either side laterally but did not appear to be expressed in the epithelium of the developing foregut (Marcus, 1929) (Fig. 5 A and B). *dpp* was expressed in large patches of ectodermal cells overlapping and dorsally adjacent to these two bands of cells enriched for *sog* expression (Fig. 5 A and B). The expression of *sog* on either side of the developing mouth led us to speculate that Dpp might provide signals that promote or inhibit mouth formation, akin to Dpp's role in regulating formation of appendages among arthropods studied. *sog* was also expressed in one endomesodermal cell on the ventral side of each of the endomesodermal pouches in each body segment (Fig. 5 D). *dpp* was expressed in segmentally iterated bands extending over each segment near the segment boundaries (Fig. 5 C and D). These bands were in the overlying ectoderm adjacent to the endomesodermal cells that expressed *sog*. Due to the banded expression pattern of *dpp* along each segment, we hypothesize that Dpp might regulate the dorsal-ventral position of future limbs in each trunk segment, similar to the role of Dpp in regulating appendage formation in arthropods and onychophorans (Goto and Hayashi, 1997; Janssen et al., 2015; Spencer et al., 1982). Alternatively or in addition, we hypothesize that Dpp might regulate cuticle patterning by guiding cuticle deposition or sites of cuticle furrowing. Finally, due to the role of ectodermal BMP in regulating mesoderm development in *D. melanogaster*, *Danio rerio*, and *M. musculus*, among other animals, and the ectodermal enrichment of *dpp*, we hypothesize that Dpp might regulate mesoderm development from overlying ectoderm (Frasch, 1995; Row et al., 2018; Staehling-Hampton et al., 1994).

We wondered whether *dpp* and *sog* expression in these regions preceded or coincided with the segmentation of the ectoderm and/or endomesoderm. They could also correspond with the future positions of the limb buds or with developing ventral trunk ganglia, both known functions of DPP signaling in other panarthropods studied (Holley et al., 1995; Janssen et al., 2015; McKay et al., 2009; Minelli et al., 2013; Spencer et al., 1982; Stollewerk, 2016; Treffkorn and Mayer, 2013; Vargas-Vila et al., 2010).

We compared expression of *dpp* and *sog* at earlier stages: elongation (18 and 19 hpl), endomesodermal pouch formation (20 hpl), and ectodermal segmentation (21 hpl) (Fig. 1 A). Lateral expression of *dpp* and *sog* were apparent by elongation (18 hpl) (Fig. 6 A). However, *dpp* was expressed in broader swaths of lateral ectoderm at elongation than at segmentation stages, and *sog* was expressed in a shorter region along the A-P axis of lateral ectoderm at elongation than at segmentation stages (Fig. 6 A-B vs C-D). Bands of *dpp* expression either coincided with or followed ectodermal segmentation (Fig. 6 D), and endomesodermal cells began expressing *sog* after endomesodermal pouch formation and during or after ectodermal segmentation (Fig. 6 C-D). Antero-lateral bands of *sog* and *dpp* near the developing mouth were apparent by elongation stages (18 hpl) (Fig. 6 A-B). These patterns indicate that *dpp* and *sog* are already expressed laterally prior to the processes of endomesodermal pouch formation and ectodermal segmentation and that the patterns of *dpp* and *sog* expression change throughout these morphological transformations.

Sog might act to restrict spread of Dpp ligand in one or multiple axes. This is complicated by the varying impacts that Sog/Chordin can have on BMP signaling and spreading (Nunes da Fonseca et al., 2010; Shimmi et al., 2005); it is possible that Sog acts to facilitate further and directed spread of Dpp protein, in conjunction with Tolloid (Tld) and Twisted Gastrulation (Tsg) (Nunes da Fonseca et al., 2010; Shimmi and O’Connor, 2003; Van Der Zee et al., 2006).

Expression of the protease *tld* is increasingly restricted along the anterior-most end of the head from 19 to 24 hpl.

Having found *dpp* expression in lateral ectoderm and in bands near segment boundaries, and antagonist *sog* expression in a more ventrally restricted domain of lateral ectoderm than *dpp*, we wondered where mRNA of the Sog protein-cleaving protease Tld was expressed, as this impacts spread of Dpp extracellularly (Nunes da Fonseca et al., 2010; Shimmi and O'Connor, 2003; Van Der Zee et al., 2006). At elongation (19 hpl), *tld* was expressed in a wide band of cells along the anterior-most end of the head (Fig. 7 A). This band was mostly non-overlapping with the bands of *sog* expression that run on either side of the developing mouth (Fig. 5, Fig. 6, and Fig. 7 A) By endomesodermal pouch formation (20 hpl), the band of cells that expressed *tld* was thinner than at 19 hpl, indicating that *tld* expression becomes more restricted and/or that the *tld*-expressing cells condense in space between these stages (Fig. 7 B). This band of *tld* expression persisted through ectodermal segmentation (24 hpl) and remained mostly non-overlapping with the two bands of *sog* expression on either side (Fig. 7 C). At ectodermal segmentation stage, *tld* expression was mostly non-overlapping with the antero-lateral patches of cells that expressed *dpp*, which were located adjacent to and slightly overlapping with the bands of *sog* expression (Fig. 7 D and Fig. 5 and Fig. 6). *tld* did not appear to be expressed in the epithelium of the developing foregut (Fig. 7 C and D). These patterns indicate that *tld* is expressed in the cells where the mouth likely develops, surrounded on either side by cells that express *sog* and *dpp*.

We speculate that, in conjunction with Sog, Tld might facilitate spreading and then release of Sog-bound Dpp either in the region of the developing mouth or internally to the mesodermal precursors – in the endomesodermal pouches of cells surrounding the foregut, which would be consistent with a possibility that Dpp might act to promote mouth development. In addition, Tld is known to function in processing collagens to mediate extracellular matrix (ECM) formation (Vadon-Le Goff et al., 2015). ECM has been shown to be important for pharyngeal morphogenesis in other ecdysozoan animals, such as the nematode *Caenorhabditis elegans* (Rasmussen et al., 2012). Therefore, it is possible that in *H. exemplaris* embryos, Tld plays a role in pharyngeal development independent of BMP.

Based on all of the results examining expression of BMP pathway genes, we conclude that the ligand-encoding gene *dpp* is expressed primarily in lateral ectoderm and in bands near segment boundaries, as well as in the head, and the BMP antagonist-encoding gene *sog* is also expressed in lateral ectoderm, less dorsally than *dpp*, including in the head, where two bands of *sog*-expressing cells are positioned between bands of *dpp*-expressing cells and flanking an anterior band of cells expressing the protease *tld*.

The expression patterns of *doc1*, *eya*, and *dpp* after segmentation of *H. exemplaris* embryos.

These expression patterns left us wondering where BMP and FGF signaling occurs during *H. exemplaris* segmentation. We turned to conserved downstream transcriptional targets of these pathways, *doc1* and *eya,* as likely markers of active signaling. *doc1* and *eya* are conserved targets of BMP signaling in other systems, such as *D. melanogaster* (Dominguez et al., 2016). Additionally, *eya* is known to be a target of FGF signaling (Ahrens and Schlosser, 2005). At ectodermal segmentation (24 hpl), *doc1* was expressed in ectoderm along the dorsal midline of the embryo, running in a band from the posterior tip of the embryo to the top of the head and then spreading into a larger region that did not extend to the anterior tip of the head (Fig. 8 A and B). *doc1* was mostly absent from internal germ layers. The expression of *doc1* in lateral ectoderm is consistent with the hypothesis that *doc1* is a target of Dpp, which has spread from lateral positions up to the dorsal ridge of the embryo, as well as from *dpp*-expressing cells on either side of the development mouth in the head. At ectodermal segmentation (24 hpl), *eya* was expressed in endomesodermal cells and the primordial germ cells and was almost entirely absent from ectoderm (Fig. 8 C and D). Expression of both *doc1* and *eya* appeared non-overlapping with the lateral ectoderm expression of *dpp* (Fig. 8). The expression of *eya* primarily in endomesoderm matches the pattern of *fgf8*-non-expressing, *fgfrl1*-expressing cells that are likely receptive to FGF signaling. We speculate it may mark endomesodermal cells in which FGF signaling is active. The expression of *eya* in primordial germ cells is consistent with the possibility that this gene

might be a target of Gbb signaling and that Gbb regulates primordial germ cell development.

Finally, between elongation and segmentation stages of *H. exemplaris* embryos, mesoderm forms. Given the known overlap of FGF and BMP in regulating mesoderm in other animals and given that these two pathways exhibit dynamic enrichment patterns between these stages along developing mesoderm, we speculate that FGF and BMP might work together to regulate mesodermal formation and/or fate specification (Row et al., 2018).

Conclusions

We have detected expression patterns for genes of components of the FGF and BMP signaling pathways during *H. exemplaris* development at segmentation stages (summarized in Fig. 9). We found that expression of the FGF ligand *fgf8* and the FGF receptor *fgfrl1* are enriched in different germ layers between elongation and ectodermal segmentation stages. *fgf8* is expressed in ectoderm at segment posteriors, and *fgfrl1* is broadly expressed in ectoderm and in underlying endomesoderm, but more enriched in the latter. The segmental expression pattern of *fgf8* precedes visible signs of ectodermal segmentation and arises before or concurrently with endomesodermal pouch formation. We also found that the BMP ligand *dpp* and antagonist *sog* are both expressed laterally and that *dpp* is expressed more dorsally than *sog*. Additionally, *sog* is expressed in bands of ectoderm on either side of the developing mouth, and *dpp* is expressed in patches slightly overlapping with and adjacent to these bands of *sog* expression. Finally, *sog* is expressed in a single ventral cell of each endomesodermal pouch, possibly in developing ventral trunk ganglia. *dpp* is expressed in bands running along segment boundaries concomitant with or near the time of ectodermal segmentation. These patterns are apparent by elongation stages and become more elaborate during the morphological process of segmentation.

Based on the expression patterns revealed, we presented hypotheses for the potential roles of FGF and BMP in *H. exemplaris* development (see Table 3 for a more comprehensive summary of hypotheses). Testing these will rely on development of techniques not yet established for this system. Our attempts to use RNAi and chemical

inhibitors to FGF (SU5402 and U0126) and BMP signaling (Dorsomorphin, DMH1, and LDN-212854) were unsuccessful (data not shown). Attempting to mark active FGF and BMP signaling, we also stained embryos using cross-reactive anti-pSMAD and anti-dpERK antibodies but did not detect specific signal (data not shown). There has been recent progress towards development of genetic tools for *H. exemplaris* by CRISPR/Cas9-based genome editing of adults with 10-20% efficient genomic deletion and via a vector-based expression system that worked mosaically in adult cells at 70-89% adult transfection efficiency and rare germline transmission (Kumagai et al., 2022; Tanaka et al., 2022). Recently, there has been progress in another tardigrade species, *Ramazzottius varieornatus*, in which CRISPR reagents injected directly into the maternal body cavity exhibited germline transmission with low efficiency (3-4%) (Kondo et al., 2024). We anticipate improvements to these techniques for efficient germline transmission are soon to follow, which would facilitate asking questions about development. Specifically, tools such as transcriptional reporters, as well as inducible protein regulation, will enable temporally specific tests of signaling pathway functions during key stages in development.

Understanding how cell signaling regulates the development of the unique tardigrade body plan will provide new information about how these conserved pathways regulate development of diverse tissue and organismal forms and ultimately how diverse body forms evolved through varied deployment of conserved signaling pathways. Expression analysis among additional tardigrade species and other animal groups will likely be valuable to grasp how nature deploys the same pathways to build widely different or convergently similar animal bodies.

Experimental Procedures

Maintaining cultures of *Hypsibius exemplaris*

Cultures were maintained as described previously (Heikes et al., 2023; McNuff, 2018).

DIC imaging of development

DIC microscopy of embryonic development was performed as previously described (Heikes et al., 2023; Heikes and Goldstein, 2018).

Gene identification and phylogenetic analyses

Genes were identified as previously described (Heikes et al., 2023). Briefly, genes were identified in a published *Hypsibius exemplaris* transcriptome (Levin et al., 2016) by tBLASTn (Altschul et al., 1990; Gerts et al., 2006; Sayers et al., 2022) using protein sequences of known homologs in *Drosophila melanogaster* from the UCSC genome browser (Kent et al., 2002). A homolog for *fgf8* could not be found in this transcriptome but was identified in another (Yoshida et al., 2017). Top hits were confirmed by reciprocal BLASTp (Sayers et al., 2022) against the *D. melanogaster* transcriptome and further confirmed through comparison of domains to the query sequence using SMART domain analysis tool in normal mode (Letunic et al., 2021; Letunic and Bork, 2018). Phylogenetic reconstructions were produced using alignments of conserved regions (either by manually-curated conserved domains or through the Gblocks program) (Castresana, 2000). Alignments were produced using Neighbor-Joining based MUSCLE alignment of curated protein sequences (Dereeper et al., 2008). Alignments were opened in Jalview to produce EPS files for figures. Alignments were also used to produce maximum likelihood phylogenetic reconstructions. Phylogenetic reconstructions were produced comparing the top hits for each query to known homologs in various species in Mega-X (500 bootstraps), as previously described (Heikes et al., 2023; Kumar et al., 2018). Accession numbers of protein sequences used in maximum likelihood reconstructions and species name abbreviations for all phylogenetic reconstructions are in Table 1.

Cloning

Genes were cloned as previously described (Heikes et al., 2023; Smith et al., 2016). Primers were designed using NCBI PrimerBLAST (Ye et al., 2012) to amplify genes by nested PCR. Primers are listed in Table 2.

Probe synthesis

RNA probes were synthesized as previously described (Heikes et al., 2023; Smith, 2018; Smith et al., 2016). Probes were labelled with either the DIG RNA labeling mix (Roche, Sigma product # 11277073910) or the Fluorescein RNA labeling mix (Roche, Sigma product # 11685619910) to facilitate double staining.

Fluorescence *in situ* hybridization

Fluorescence *in situ* hybridization (FISH) was performed using the Tyramide Signal Amplification kit from Akoya Biosciences, as previously described (Heikes et al., 2023), with the addition of a second round of antibody and signal amplification for double FISH. The added steps for double FISH performed were as follows, starting with the end of the tyramide signal amplification (steps 37-42) in the protocol previously published (Heikes et al., 2023). Embryos were washed in pre-heated Solution X for 20 minutes at 60°C (final concentrations: 50% formamide, 2x SSC, 1% SDS, diluted in DEPC-treated water) to inactivate peroxidase activity from the anti-DIG-POD antibody. Embryos were then washed four times quickly in 0.5x PBTw at room temperature. The protocol was then repeated starting from step 34 (Heikes et al., 2023) through to the end of the protocol, with the exception that anti-FITC-POD antibody was used to detect FITC-labelled RNA probes, instead of the anti-DIG-POD antibody used in the first round of detection. For both antibody incubations, a concentration of 1:500 antibody:blocking buffer was used. DIG-labelled probes were amplified with Cy3 amplification reagent (Akoya product # NEL744001KT) and FITC-labelled probes were amplified with Cy5 amplification reagent (Akoya product # NEL745001KT).

Fluorescence microscopy

FISH-stained embryos were imaged on a Zeiss LSM 710 microscope with a Plan-Neofluor 100x/1.3 oil Iris objective or a Zeiss LSM 880 microscopy with fast Airyscan detector and a Plan-Apochromat 63x/1.4 oil DIC objective. DAPI signal was excited with a 405 nm laser and collected between 411 and 543 nm. Cy3 signal was excited with a 560 nm laser and collected between 561 and 620 nm. Cy5 signal was excited with a 633 nm laser and collected between 639 and 750 nm. Images were opened in FIJI or Zen Black edition for image analysis. Minimum and Maximum displayed values were linearly adjusted in FIJI or Zen Black edition, and images were exported to scale in PNG format for cropping and annotation. Figures were made in Adobe Illustrator. Scale bars were added in Illustrator by pixel scale. DAPI stained DNA signal is displayed as blue in all figures. Cy3-amplified DIG-labelled probe signal is displayed in green in all figures, except for single-channel images, which are displayed in grayscale. Cy5-amplified FITC-labelled probe signal is displayed as magenta in all figures. Figure images are

representative of multiple samples across independent rounds of staining, with sample numbers listed in each legend. Anterior is up in all images. Large dashed lines in figures indicate the boundary between the anterior and posterior of embryos.

Curating diagrams of development

Diagrams of development were hand-drawn on a Samsung Galaxy S8 tablet in the Concepts app, using fluorescence images to trace outlines and expression patterns.

Acknowledgements

We thank members of the Goldstein lab, past and present, for ideas and promoting a supportive environment conducive to research with an emerging model. In particular, we thank Frank Smith and members of the Smith lab for scientific discussions and for discussing unpublished results freely. We thank the UNC Biology Department, especially Tony Purdue and Nat Prunet for technical assistance in the UNC Biology microscopy core. We thank Dr. Amy Maddox, Dr. Amy Gladfelter, Dr. Greg Wray, and Dr. Christina Burch for helpful feedback on the manuscript and/or scientific discussions.

References:

Ahrens, K., Schlosser, G., 2005. Tissues and signals involved in the induction of placodal Six1 expression in Xenopus laevis. Dev. Biol. 288, 40–59. https://doi.org/10.1016/j.ydbio.2005.07.022

Akam, M., 1995. Hox genes and the evolution of diverse body plans. Philos. Trans. R. Soc. B Biol. Sci. 349, 313–319. https://doi.org/10.1098/rstb.1995.0119

Alberga, A., Boulay, J., Kempe, E., Dennefeld, C., Haenlin, M., 1991. The snail gene required for mesoderm formation in Drosophila is expressed dynamically in derivatives of all three germ layers. Development 111, 983–992. https://doi.org/doi.org/10.1242/dev.111.4.983

Altschul, S.F., Gish, W., Miller, W., Myers, E.W., Lipman, D.J., 1990. Basic local alignment search tool. J. Mol. Biol. 215, 403–410. https://doi.org/10.1016/S0022-2836(05)80360-2

Andrikou, C., Hejnol, A., 2021. FGF signaling acts on different levels of mesoderm development within Spiralia. Dev. 148. https://doi.org/10.1242/DEV.196089

Angelini, D.R., Kaufman, T.C., 2005. Functional analyses in the milkweed bug Oncopeltus fasciatus (Hemiptera) support a role for Wnt signaling in body segmentation but not appendage development. Dev. Biol. 283, 409–423. https://doi.org/10.1016/j.ydbio.2005.04.034

Beermann, A., Schröder, R., 2008. Sites of Fgf signalling and perception during embryogenesis of the beetle Tribolium castaneum. Dev. Genes Evol. 218, 153–167. https://doi.org/10.1007/s00427-007-0192-x

Bertrand, E., Chartrand, P., Schaefer, M., Shenoy, S.M., Singer, R.H., Long, R.M., 1998. Localization of ASH1 mRNA particles in living yeast. Mol. Cell 2, 437–445. https://doi.org/10.1016/S1097-2765(00)80143-4

Cano, A., Pérez-moreno, M.A., Rodrigo, I., Locascio, A., Blanco, M.J., del Barrio, M.G., Portillo, F., Nieto, M.A., 2000. The transcription factor Snail controls epithelial – mesenchymal

transitions by repressing E-cadherin expression. Nat. Cell Biol. 2, 76–83. https://doi.org/https://doi.org/10.1038/35000025

Castresana, J., 2000. Selection of conserved blocks from multiple alignments for their use in phylogenetic analysis. Mol. Biol. Evol. 17, 540–552. https://doi.org/10.1093/oxfordjournals.molbev.a026334

Chavarria, R.A., Game, M., Arbelaez, B., Ramnarine, C., Snow, Z.K., Smith, F.W., 2021. Extensive loss of Wnt genes in Tardigrada. BMC Ecol. Evol. 21, 1–21. https://doi.org/10.1186/s12862-021-01954-y

Chopra, V.S., Levine, M., 2009. Combinatorial patterning mechanisms in the Drosophila embryo. Briefings Funct. Genomics Proteomics 8, 243–249. https://doi.org/10.1093/bfgp/elp026

Dereeper, A., Guignon, V., Blanc, G., Audic, S., Buffet, S., Chevenet, F., Dufayard, J.F., Guindon, S., Lefort, V., Lescot, M., Claverie, J.M., Gascuel, O., 2008. Phylogeny.fr: robust phylogenetic analysis for the non-specialist. Nucleic Acids Res. 36, 465–469. https://doi.org/10.1093/nar/gkn180

DeVore, D.L., Horvitz, H.R., J.Stern, M., 1995. An FGF receptor signaling pathway is required for the normal cell migrations of the sex myoblasts in C. elegans hermaphrodites. Cell 83, 611–620. https://doi.org/10.1016/0092-8674(95)90101-9

Dominguez, C., Zuñiga, A., Hanna, P., Hodar, C., Gonzalez, M., Cambiazo, V., 2016. Target genes of Dpp/BMP signaling pathway revealed by transcriptome profiling in the early D. melanogaster embryo. Gene 592, 191–200. https://doi.org/10.1016/j.gene.2016.07.015

Donoughe, S., Nakamura, T., Ewen-Campen, B., Green, D.A., Henderson, L., Extavour, C.G., 2014. BMP signaling is required for the generation of primordial germ cells in an insect. Proc. Natl. Acad. Sci. U. S. A. 111, 4133–4138. https://doi.org/10.1073/pnas.1400525111

Erives, A., Corbo, J.C., Levine, M., 1998. Lineage-specific regulation of the Ciona snail gene in

the embryonic mesoderm and neuroectoderm. Dev. Biol. 194, 213–225. https://doi.org/10.1006/dbio.1997.8810

Ewen-Campen, B., Donoughe, S., Clarke, D.N., Extavour, C.G., 2013. Article Germ Cell Specification Requires Zygotic Mechanisms Rather Than Germ Plasm in a Basally Branching Insect. Curr. Biol. 23, 835–842. https://doi.org/10.1016/j.cub.2013.03.063

Fan, T.P., Ting, H.C., Yu, J.K., Su, Y.H., 2018. Reiterative use of FGF signaling in mesoderm development during embryogenesis and metamorphosis in the hemichordate Ptychodera flava. BMC Evol. Biol. 18, 1–16. https://doi.org/10.1186/s12862-018-1235-9

Franke, F.A., Mayer, G., 2014. Controversies surrounding segments and parasegments in onychophora: Insights from the expression patterns of four “segment polarity genes” in the peripatopsid euperipatoides rowelli. PLoS One 9, 1–31. https://doi.org/10.1371/journal.pone.0114383

Frasch, M., 1995. Induction of visceral and cardiac mesoderm by ectodermal dpp in the early drosophila embryo. Nature 374, 464–467. https://doi.org/10.1038/374464a0

Gabriel, W.N., 2007. The tardigrade Hypsibius dujardini as a new model for studies on the evolution of development. University of North Carolina at Chapel Hill. https://doi.org/doi.org/10.17615/nfdc-g862

Gabriel, W.N., Goldstein, B., 2007. Segmental expression of Pax3 / 7 and Engrailed homologs in tardigrade development. Dev. Genes Evol. 217, 421–433. https://doi.org/10.1007/s00427-007-0152-5

Gabriel, W.N., Mcnuff, R., Patel, S.K., Gregory, T.R., Jeck, W.R., Jones, C.D., Goldstein, B., 2007. The tardigrade Hypsibius dujardini, a new model for studying the evolution of development. Dev. Biol. 312, 545–559. https://doi.org/10.1016/j.ydbio.2007.09.055

Game, M., Smith, F.W., 2020. Loss of intermediate regions of perpendicular body axes contributed to miniaturization of tardigrades. Proc. R. Soc. B Biol. Sci. 287.

https://doi.org/10.1098/rspb.2020.1135

Garcia, H.G., Tikhonov, M., Lin, A., Gregor, T., 2013. Quantitative Imaging of Transcription in Living Drosophila Embryos Links Polymerase Activity to Patterning. Curr. Biol. 23, 2140–2145. https://doi.org/10.1016/j.cub.2013.08.054

Gerts, E.M., Yu, Y.K., Agarwala, R., Schäffer, A.A., Altschul, S.F., 2006. Composition-based statistics and translated nucleotide searches: Improving the TBLASTN module of BLAST. BMC Biol. 4, 1–14. https://doi.org/10.1186/1741-7007-4-41

Giribet, G., Edgecombe, G.D., 2017. Current understanding of Ecdysozoa and its internal phylogenetic relationships. Integr. Comp. Biol. 57, 455–466. https://doi.org/10.1093/icb/icx072

Goldstein, B., 2018. The Emergence of the Tardigrade Hypsibius exemplaris as a Model System. Cold Spring Harb. Protoc. 859–866. https://doi.org/10.1101/pdb.emo102301

Goldstein, B., Blaxter, M., 2002. Quick guide Tardigrades. Curr. Biol. 12, 475. https://doi.org/10.1016/s0960-9822(02)00959-4

Goto, S., Hayashi, S., 1997. Specification of the embryonic limb primordium by graded activity of Decapentaplegic. Development 124, 125–132. https://doi.org/10.1242/dev.124.1.125

Green, S.A., Norris, R.P., Terasak, M., Lowe, C.J., 2013. FGF signaling induces mesoderm in the hemichordate Saccoglossus kowalevskii. Dev. 140, 1024–1033. https://doi.org/10.1242/dev.083790

Gross, V., Treffkorn, S., Reichelt, J., Epple, L., Lüter, C., Mayer, G., 2019. Miniaturization of tardigrades (water bears): Morphological and genomic perspectives. Arthropod Struct. Dev. 48, 12–19. https://doi.org/10.1016/j.asd.2018.11.006

Gryzik, T., Muller, H.-A.J., 2004. FGF8-like1 and FGF8-like2 Encode Putative Ligands of the FGF Receptor Htl and Are Required for Mesoderm Migration in the Drosophila Gastrula. Curr. Biol. 14, 659–667. https://doi.org/10.1016/j.cub.2004.03.058

Hamaratoglu, F., Affolter, M., Pyrowolakis, G., 2014. Dpp/BMP signaling in flies: From molecules to biology. Semin. Cell Dev. Biol. 32, 128–136. https://doi.org/10.1016/j.semcdb.2014.04.036

Hannibal, R.L., Price, A.L., Parchem, R.J., Patel, N.H., 2012. Analysis of snail genes in the crustacean parhyale hawaiensis: Insight into snail gene family evolution. Dev. Genes Evol. 222, 139–151. https://doi.org/10.1007/s00427-012-0396-6

Heikes, K.L., Game, M., Smith, F.W., Goldstein, B., 2023. The embryonic origin of primordial germ cells in the tardigrade Hypsibius exemplaris. Dev. Biol. 497, 42–58. https://doi.org/10.1016/j.ydbio.2023.02.008

Heikes, K.L., Goldstein, B., 2018. Live Imaging of Tardigrade Embryonic Development by Differential Interference Contrast Microscopy. Cold Spring Harb. Protoc. https://doi.org/10.1101/pdb.prot102335

Hejnol, A., Schnabel, R., 2005. The eutardigrade Thulinia stephaniae has an indeterminate development and the potential to regulate early blastomere ablations 1349–1361. https://doi.org/10.1242/dev.01701

Hemavathy, K., Meng, X., Ip, Y.T., 1997. Differential regulation of gastrulation and neuroectodermal gene expression by Snail in the Drosophila embryo. Development 124, 3683–3691. https://doi.org/10.1242/dev.124.19.3683

Hogvall, M., Budd, G.E., Janssen, R., 2018. Gene expression analysis of potential morphogen signalling modifying factors in Panarthropoda. Evodevo 9, 1–24. https://doi.org/10.1186/s13227-018-0109-y

Hogvall, M., Schönauer, A., Budd, G.E., McGregor, A.P., Posnien, N., Janssen, R., 2014. Analysis of the Wnt gene repertoire in an onychophoran provides new insights into the evolution of segmentation. Evodevo 5, 1–15. https://doi.org/10.1186/2041-9139-5-14

Holley, S.A., Jackson, P.D., Sasai, Y., Lu, B., Robertis, E.M. De, Hoffmann, F.M., Ferguson,

E.L., 1995. A conserved system for dorsal-ventral patterning in insects and vertebrates involving sog and chordin. Nature 376, 249–253. https://doi.org/doi: 10.1038/376249a0

Howard, R.J., Giacomelli, M., Lozano-Fernandez, J., Edgecombe, G.D., Fleming, J.F., Kristensen, R.M., Ma, X., Olesen, J., Sørensen, M. V., Thomsen, P.F., Wills, M.A., Donoghue, P.C.J., Pisani, D., 2022. The Ediacaran origin of Ecdysozoa: integrating fossil and phylogenomic data. J. Geol. Soc. London. 179. https://doi.org/10.1144/jgs2021-107

Huang, P., Stern, M.J., 2005. FGF signaling in flies and worms: More and more relevant to vertebrate biology. Cytokine Growth Factor Rev. 16, 151–158. https://doi.org/10.1016/j.cytogfr.2005.03.002

Hughes, C.L., Kaufman, T.C., 2002. Hox genes and the evolution of the arthropod body plan. Evol. Dev. 4, 459–499. https://doi.org/10.1046/j.1525-142X.2002.02034.x

Janssen, R., 2017. A molecular view of onychophoran segmentation. Arthropod Struct. Dev. 46, 341–353. https://doi.org/10.1016/j.asd.2016.10.004

Janssen, R., Eriksson, B.J., Tait, N.N., Budd, G.E., 2014. Onychophoran Hox genes and the evolution of arthropod Hox gene expression. Front. Zool. 11, 1–11. https://doi.org/10.1186/1742-9994-11-22

Janssen, R., Jörgensen, M., Prpic, N.M., Budd, G.E., 2015. Aspects of dorso-ventral and proximo-distal limb patterning in onychophorans. Evol. Dev. 17, 21–33. https://doi.org/10.1111/ede.12107

Kadam, S., Ghosh, S., Stathopoulos, A., 2012. Synchronous and symmetric migration of Drosophila caudal visceral mesoderm cells requires dual input by two FGF ligands. Development 139, 699–708. https://doi.org/10.1242/dev.068791

Kainz, F., 2009. PhD Thesis. Gonville & Caius College, University of Cambridge, Cambridge.

Kent, W.J., Sugnet, C.W., Furey, T.S., Roskin, K.M., Pringle, T.H., Zahler, A.M., Haussler, and D., 2002. The Human Genome Browser at UCSC. Genome Res. 12, 996–1006.

https://doi.org/10.1101/gr.229102

Kimelman, D., Kirschner, M., 1987. Synergistic induction of mesoderm by FGF and TGF-β and the identification of an mRNA coding for FGF in the early xenopus embryo. Cell 51, 869–877. https://doi.org/10.1016/0092-8674(87)90110-3

Klingseisen, A., Clark, I.B.N., Gryzik, T., Müller, H.J., 2009. Differential and overlapping functions of two closely related Drosophila FGF8-like growth factors in mesoderm development. Development 136, 2393–2402. https://doi.org/10.1242/dev.035451

Kondo, K., Tanaka, A., Kunieda, T., 2024. Single-step generation of homozygous knockout/knock-in individuals in an extremotolerant parthenogenetic tardigrade using DIPA-CRISPR. PLoS Genet. 20. https://doi.org/10.1371/journal.pgen.1011298

Kumagai, H., Kondo, K., Kunieda, T., 2022. Application of CRISPR/Cas9 system and the preferred no-indel end-joining repair in tardigrades. Biochem. Biophys. Res. Commun. 623, 196–201. https://doi.org/10.1016/j.bbrc.2022.07.060

Kumar, S., Stecher, G., Li, M., Knyaz, C., Tamura, K., 2018. MEGA X: Molecular evolutionary genetics analysis across computing platforms. Mol. Biol. Evol. 35, 1547–1549. https://doi.org/10.1093/molbev/msy096

Lawson, K.A., Dunn, N.R., Roelen, B.A.J., Zeinstra, L.M., Davis, A.M., Wright, C.V.E., Korving, J.P.W.F.M., Hogan, B.L.M., 1999. Bmp4 is required for the generation of primordial germ cells in the mouse embryo. Genes Dev. 13, 424–436. https://doi.org/10.1101/gad.13.4.424

Leptin, M., 1991. twist and snail as positive and negative regulators during Drosophila mesoderm development. Genes Dev. 5, 1568–1576. https://doi.org/10.1101/gad.5.9.1568

Letunic, I., Bork, P., 2018. 20 years of the SMART protein domain annotation resource. Nucleic Acids Res. 46, D493–D496. https://doi.org/10.1093/nar/gkx922

Letunic, I., Khedkar, S., Bork, P., 2021. SMART: Recent updates, new developments and status in 2020. Nucleic Acids Res. 49, D458–D460. https://doi.org/10.1093/nar/gkaa937

Levin, M., Anavy, L., Cole, A.G., Winter, E., Mostov, N., Khair, S., Senderovich, N., Kovalev, E., Silver, D.H., Feder, M., Fernandez-Valverde, S.L., Nakanishi, N., Simmons, D., Simakov, O., Larsson, T., Liu, S.-Y., Jerafi-Vider, A., Yaniv, K., Ryan, J.F., Martindale, M.Q., Rink, J.C., Arendt, D., Degnan, S.M., Degnan, B.M., Hashimshony, T., Yanai, I., 2016. The mid-developmental transition and the evolution of animal body plans. Nature 531, 637–641. https://doi.org/10.1038/nature16994

Lochab, A.K., Extavour, C.G., 2017. Bone Morphogenetic Protein (BMP) signaling in animal reproductive system development and function. Dev. Biol. 427, 258–269. https://doi.org/10.1016/j.ydbio.2017.03.002

Lucas, T., Ferraro, T., Roelens, B., De Las Heras Chanes, J., Walczak, A.M., Coppey, M., Dostatni, N., 2013. Live Imaging of Bicoid-Dependent Transcription in Drosophila Embryos. Curr. Biol. 23, 2135–2139. https://doi.org/10.1016/j.cub.2013.08.053

Luo, K., 2017. Signaling Cross Talk between TGF-b / Smad and Other Signaling Pathways. Cold Spring Harb. Persepctives Biol. 9, 1–28. https://doi.org/10.1101/cshperspect.a022137

Mapalo, M.A., Game, M., Smith, F.W., Ortega-Hernández, J., 2024. Expression of distal limb patterning genes in Hypsibius exemplaris indicate regionalization and suggest distal identity of tardigrade legs. Evodevo 15, 1–15. https://doi.org/10.1186/s13227-024-00235-1

Marcus, E., 1929. Zur Embryologie der Tardigraden. Zool. Jahrbücher, Abteilung für Anat. und Ontog. der Tiere 50, 333–384. https://doi.org/10.23736/S0392-9590.16.03730-5

Matus, D.Q., Thomsen, G.H., Martindale, M.Q., 2007. FGF signaling in gastrulation and neural development in Nematostella vectensis, an anthozoan cnidarian. Dev. Genes Evol. 217, 137–148. https://doi.org/10.1007/s00427-006-0122-3

Mayer, G., Kato, C., Quast, B., Chisholm, R.H., Landman, K.A., Quinn, L.M., 2010. Growth patterns in Onychophora (velvet worms): Lack of a localised posterior proliferation zone. BMC Evol. Biol. 10, 1–12. https://doi.org/10.1186/1471-2148-10-339

McGregor, A.P., Pechmann, M., Schwager, E.E., Feitosa, N.M., Kruck, S., Aranda, M., Damen, W.G.M., 2008. Wnt8 Is Required for Growth-Zone Establishment and Development of Opisthosomal Segments in a Spider. Curr. Biol. 18, 1619–1623. https://doi.org/10.1016/j.cub.2008.08.045

McKay, D.J., Estella, C., Mann, R.S., 2009. The origins of the Drosophila leg revealed by the cis-regulatory architecture of the Distalless gene. Development 136, 61–71. https://doi.org/10.1242/dev.029975

McNuff, R., 2018. Laboratory Culture of Hypsibius exemplaris. Cold Spring Harb. Protoc. 867–870. https://doi.org/10.1101/pdb.prot102319

Minelli, A., Fusco, G., Boxshall, G., 2013. Arthropod biology and evolution: Molecules, development, morphology. Arthropod Biol. Evol. Mol. Dev. Morphol. 1–532. https://doi.org/10.1007/978-3-642-36160-9

Miyawaki, K., Mito, T., Sarashina, I., Zhang, H., Shinmyo, Y., Ohuchi, H., Noji, S., 2004. Involvement of Wingless/Armadillo signaling in the posterior sequential segmentation in the cricket, Gryllus bimaculatus (Orthoptera), as revealed by RNAi analysis. Mech. Dev. 121, 119–130. https://doi.org/10.1016/j.mod.2004.01.002

Morisato, D., Anderson, K. V., 1995. Signaling pathways that establish the dorsal-ventral pattern of the Drosophila embryo. Annu. Rev. Genet. 29, 371–399. https://doi.org/10.1146/annurev.genet.29.1.371

Muha, V., Müller, H.A.J., 2013. Functions and mechanisms of fibroblast growth factor (FGF) signalling in Drosophila melanogaster. Int. J. Mol. Sci. 14, 5920–5937. https://doi.org/10.3390/ijms14035920

Mullins, M.C., 1998. Holy Tolloido: Tolloid cleaves SOG/Chordin to free DPP/BMPs. Trends Genet. 14, 127–129. https://doi.org/10.1016/S0168-9525(98)01431-0

Nakamura, T., Extavour, C.G., 2016. The transcriptional repressor Blimp-1 acts downstream of

BMP signaling to generate primordial germ cells in the cricket Gryllus bimaculatus. Development 143, 255–263. https://doi.org/10.1242/dev.127563

Nakayama, T., Cui, Y., Christian, J.L., 2000. Regulation of BMP / Dpp signaling during embryonic development. Cell. Mol. Life Sci. 57, 943–956. https://doi.org/10.1007/PL00000736

Nunes da Fonseca, R., van der Zee, M., Roth, S., 2010. Evolution of extracellular Dpp modulators in insects: The roles of tolloid and twisted-gastrulation in dorsoventral patterning of the Tribolium embryo. Dev. Biol. 345, 80–93. https://doi.org/10.1016/j.ydbio.2010.05.019

Pechmann, M., Benton, M.A., Kenny, N.J., Posnien, N., Roth, S., 2017. A novel role for Ets4 in axis specification and cell migration in the spider Parasteatoda tepidariorum. Elife 6, 1–20. https://doi.org/10.7554/eLife.27590

Peel, A.D., Chipman, A.D., Akam, M., 2005. Arthropod segmentation: Beyond the Drosophila paradigm. Nat. Rev. Genet. 6, 905–916. https://doi.org/10.1038/nrg1724

Pires-daSilva, A., Sommer, R.J., 2003. THE EVOLUTION OF SIGNALLING PATHWAYS IN ANIMAL DEVELOPMENT. Nat. Rev. Genet. 4, 39–49. https://doi.org/10.1038/nrg977

Ramel, M.C., Hill, C.S., 2012. Spatial regulation of BMP activity. FEBS Lett. 586, 1929–1941. https://doi.org/10.1016/j.febslet.2012.02.035

Rasmussen, J.P., Reddy, S.S., Priess, J.R., 2012. Laminin is required to orient epithelial polarity in the C. elegans pharynx. Development 139, 2050–2060. https://doi.org/10.1242/dev.078360

Röttinger, E., Saudemont, A., Duboc, V., Besnardeau, L., McClay, D., Lepage, T., 2008. Erratum: FGF signals guide migration of mesenchymal cells, control skeletal morphogenesis and regulate gastrulation during sea urchin development (Development vol. 135 (353-365)). Development 135, 785. https://doi.org/10.1242/dev.020016

Row, R.H., Pegg, A., Kinney, B.A., Farr, G.H., Maves, L., Lowell, S., Wilson, V., Martin, B.L., 2018. BMP and FGF signaling interact to pattern mesoderm by controlling basic helix-loop-helix transcription factor activity. Elife 7, 1–27. https://doi.org/10.7554/eLife.31018

Sayers, E.W., Bolton, E.E., Brister, J.R., Canese, K., Chan, J., Comeau, D.C., Connor, R., Funk, K., Kelly, C., Kim, S., Madej, T., Marchler-Bauer, A., Lanczycki, C., Lathrop, S., Lu, Z., Thibaud-Nissen, F., Murphy, T., Phan, L., Skripchenko, Y., Tse, T., Wang, J., Williams, R., Trawick, B.W., Pruitt, K.D., Sherry, S.T., 2022. Database resources of the national center for biotechnology information. Nucleic Acids Res. 50, D20–D26. https://doi.org/10.1093/nar/gkab1112

Schill, R.O., 2018. Water Bears: The Biology of Tardigrades. Springer. https://doi.org/10.1007/978-3-319-95702-9

Sharma, R., Beer, K., Iwanov, K., Schmöhl, F., Beckmann, P.I., Schröder, R., 2015. The single fgf receptor gene in the beetle Tribolium castaneum codes for two isoforms that integrate FGF8-and Branchless-dependent signals. Dev. Biol. 402, 264–275. https://doi.org/10.1016/j.ydbio.2015.04.001

Sharma, R., Beermann, A., Schröder, R., 2013. FGF signalling controls anterior extraembryonic and embryonic fate in the beetle Tribolium. Dev. Biol. 381, 121–133. https://doi.org/10.1016/j.ydbio.2013.05.031

Shimmi, O., O'Connor, M.B., 2003. Physical properties of Tld, Sog, Tsg and Dpp protein interactions are predicted to help create a sharp boundary in Bmp signals during dorsoventral patterning of the Drosophila embryo. Development 130, 4673–4682. https://doi.org/10.1242/dev.00684

Shimmi, O., Umulis, D., Othmer, H., Connor, M.B.O., 2005. Facilitated Transport of a Dpp / Scw Heterodimer by Sog / Tsg Leads to Robust Patterning of the Drosophila Blastoderm Embryo 120, 873–886. https://doi.org/10.1016/j.cell.2005.02.009

Simpson, P., 1983. Maternal-zygotic gene interactions during formation o f t h e dorsoventral pattern in drosophila embryos. Genetics 105, 615–632. https://doi.org/doi.org/10.1093/genetics/105.3.615

Smith, F.W., 2018. Embryonic In Situ Hybridization for the Tardigrade Hypsibius exemplaris. Cold Spring Harb. Protoc. 891–899. https://doi.org/10.1101/pdb.prot102350

Smith, F.W., Boothby, T.C., Giovannini, I., Rebecchi, L., Jockusch, E.L., Goldstein, B., 2016. The Compact Body Plan of Tardigrades Evolved by the Loss of a Large Body Region. Curr. Biol. 26, 224–229. https://doi.org/10.1016/j.cub.2015.11.059

Smith, F.W., Cumming, M., Goldstein, B., 2018. Analyses of nervous system patterning genes in the tardigrade Hypsibius exemplaris illuminate the evolution of panarthropod brains. Evodevo. https://doi.org/10.1186/s13227-018-0106-1

Smith, F.W., Game, M., Mapalo, M.A., Chavarria, R.A., Harrison, T.R., Janssen, R., 2023. Developmental and genomic insight into the origin of the tardigrade body plan. Evol. Dev. 1–18. https://doi.org/10.1111/ede.12457

Smith, F.W., Goldstein, B., 2017. Segmentation in Tardigrada and diversification of segmental patterns in Panarthropoda. Arthropod Struct. Dev. 46, 328–340. https://doi.org/10.1016/j.asd.2016.10.005

Spencer, F.A., Hoffmann, F.M., Gelbart, W.M., 1982. Decapentaplegic: A gene complex affecting morphogenesis in Drosophila melanogaster. Cell 28, 451–461. https://doi.org/10.1016/0092-8674(82)90199-4

Staehling-Hampton, K., Hoffmann, F.M., Baylies, M.K., Rushton, E., Bate, M., 1994. dpp induces mesodermal gene expression in Drosophila. Nature 372, 783–786. https://doi.org/10.1038/372783a0

Stathopoulos, A., Tam, B., Ronshaugen, M., Frasch, M., Levine, M., 2004. Pyramus and thisbe: FGF genes that pattern the mesoderm of Drosophila embryos. Genes Dev. 18, 687–699.

https://doi.org/10.1101/gad.1166404

Stepanik, V., Sun, J., Stathopoulos, A., 2020. FGF Pyramus Has a Transmembrane Domain and Cell-Autonomous Function in Polarity. Curr. Biol. 30, 3141-3153.e5. https://doi.org/10.1016/j.cub.2020.06.006

Stollewerk, A., 2016. A flexible genetic toolkit for arthropod neurogenesis. Philos. Trans. R. Soc. B Biol. Sci. 371. https://doi.org/10.1098/rstb.2015.0044

Suzuki, A., Thies, R.S., Yamaji, N., Song, J.J., Wozney, J.M., Murakami, K., Ueno, N., 1994. A truncated bone morphogenetic protein receptor affects dorsal-ventral patterning in the early Xenopus embryo. Proc. Natl. Acad. Sci. U. S. A. 91, 10255–10259. https://doi.org/10.1073/pnas.91.22.10255

Tanaka, S., Aoki, K., Arakawa, K., 2022. in vivo expression vector derived from anhydrobiotic tardigrade genome enables live imaging in Eutardigrada. PNAS 120. https://doi.org/doi.org/10.1073/pnas.2216739120

Telford, M.J., Bourlat, S.J., Economou, A., Papillon, D., Rota-Stabelli, O., 2008. The evolution of the Ecdysozoa. Philos. Trans. R. Soc. B Biol. Sci. 363, 1529–1537. https://doi.org/10.1098/rstb.2007.2243

Treffkorn, S., Mayer, G., 2013. Expression of the decapentaplegic ortholog in embryos of the onychophoran Euperipatoides rowelli. Gene Expr. Patterns 13, 384–394. https://doi.org/10.1016/j.gep.2013.07.004

Vadon-Le Goff, S., Hulmes, D.J.S., Moali, C., 2015. BMP-1/tolloid-like proteinases synchronize matrix assembly with growth factor activation to promote morphogenesis and tissue remodeling. Matrix Biol. 44–46, 14–23. https://doi.org/10.1016/j.matbio.2015.02.006

Van Der Zee, M., Stockhammer, O., Von Levetsow, C., Nunes Da Fonseca, R., Roth, S., 2006. Sog/chordin is required for ventral-to-dorsal Dpp/BMP transport and head formation in a short germ insect. Proc. Natl. Acad. Sci. U. S. A. 103, 16307–16312.

https://doi.org/10.1073/pnas.0605154103

Vargas-Vila, M.A., Hannibal, R.L., Parchem, R.J., Liu, P.Z., Patel, N.H., 2010. A prominent requirement for single-minded and the ventral midline in patterning the dorsoventral axis of the crustacean Parhyale hawaiensis. Development 137, 3469–3476. https://doi.org/10.1242/dev.055160

Wang, R., Leite, D.J., Karadas, L., Schiffer, P.H., Pechmann, M., 2023. FGF signalling is involved in cumulus migration in the common house spider Parasteatoda tepidariorum. Dev. Biol. 494, 35–45. https://doi.org/10.1016/j.ydbio.2022.11.009

Wijesena, N., Simmons, D.K., Martindale, M.Q., 2017. Antagonistic BMP-cWNT signaling in the cnidarian Nematostella vectensis reveals insight into the evolution of mesoderm. Proc. Natl. Acad. Sci. U. S. A. 114, E5608–E5615. https://doi.org/10.1073/pnas.1701607114

Winnier, G., Blessing, M., Labosky, P.A., Brigid, L.M.H., 1995. Bone morphogenetic protein-4 is required for mesoderm formation and patterning in the mouse. Genes Dev. 9, 2105–2116. https://doi.org/10.1101/gad.9.17.2105

Wu, B., Chao, J.A., Singer, R.H., 2012. Fluorescence fluctuation spectroscopy enables quantitative imaging of single mRNAs in living cells. Biophys. J. 102, 2936–2944. https://doi.org/10.1016/j.bpj.2012.05.017

Ye, J., Coulouris, G., Zaretskaya, I., Cutcutache, I., Rozen, S., Madden, T.L., 2012. Primer-BLAST: A tool to design target-specific primers for polymerase chain reaction Jian. BMC Bioinformatics 13. https://doi.org/10.1186/1471-2105-13-134

York, J.R., Zehnder, K., Yuan, T., Lakiza, O., McCauley, D.W., 2019. Evolution of Snail-mediated regulation of neural crest and placodes from an ancient role in bilaterian neurogenesis. Dev. Biol. 453, 180–190. https://doi.org/10.1016/j.ydbio.2019.06.010

Yoshida, Y., Koutsovoulos, G., Laetsch, D.R., Stevens, L., Kumar, S., Horikawa, D.D., Ishino, K., Komine, S., Kunieda, T., Tomita, M., Blaxter, M., Arakawa, K., 2017. Comparative

genomics of the tardigrades Hypsibius dujardini and Ramazzottius varieornatus, PLoS Biology. https://doi.org/10.1371/journal.pbio.2002266

Tables and Figures

Table 1 Accession numbers used for phylogenetic analysis

Accession Numbers for ML Protein Phylogenetic Reconstructions					
Species Abbrev.	**FGF8-like**	**Source**	**Sequence ID**	**Translation?**	**Species Name**
He	Fgf8	GenBank PRJNA360553	BV898_11515_t01	expasy	*Hypsibius exemplaris*
Dm	Ths	UCSC	NP_610701		*Drosophila melanogaster*
Ce	Egl-17	UCSC	NP_508107		*Caenorhabditis elegans*
Hv	FGF8	GenBank	XP_012554564.1		*Hydra vulgaris*
Sk	Fgf8	GenBank	ADB22412.1		*Saccoglossus kowalevskii*
Dr	Fgf8	GenBank	AAB82614.1		*Danio rerio*
Hs	Fgf8	GenBank	NP_149353.1		*Homo sapiens*
Bf	Fgf8	GenBank	XP_035674358.1		*Branchiostoma floridae*
Ci	Fgf8/17/18	GenBank	NP_001027648.1		*Ciona intestinalis*
Pf	Fgf8/17/18	GenBank	AKZ18202.1		*Ptychodera flava*
Nv	FGF8a	GenBank	ABN70836.1		*Nematostella vectensis*
Tt	Fgf8/17/18	GenBank	ALS19758.1		*Terebratalia transversa*
Na	Fgf8/17/18	GenBank	ALS19767.1		*Novocrania anomala*
Ph	Fgf8/17/18	GenBank	QUP08116.1		*Phoronopsis harmeri*
Species Abbrev.	**9/16/20 Family of FGFs**	**Source**	**Sequence ID**	**Translation?**	**Species Name**
Dm	Pyr	UCSC	NP_001097275		*Drosophila melanogaster*
Dm	Bnl	UCSC	NP_732452		*Drosophila melanogaster*
Ce	Let-756	UCSC	NP_498403		*Caenorhabditis elegans*
Nv	FGF9	GenBank	XP_032228973.1		*Nematostella vectensis*

Bf	FGF9	GenBank	XP_035675604.1		*Branchiostoma floridae*
Tt	FGF9/16/20	GenBank	QUP08106.1		*Terebratalia transversa*
Na	FGF9/16/20	GenBank	QUP08110.1		*Novocrania anomala*
Ph	FGF9/16/20	GenBank	QUP08115.1		*Phoronopsis harmeri*
Hv	FGF9	GenBank	AND74489.1		*Hydra vulgaris*
Ci	FGF9/16/20	GenBank	NP_001027649.1		*Ciona intestinalis*
Hs	FGF9	GenBank	NP_002001.1		*Homo sapiens*
Dr	FGF9	GenBank	XP_009302933.1		*Danio rerio*
Sk	FGF9	GenBank	NP_001161538		*Saccoglossus kowalevskii*
Species Abbrev.	**FGF Receptor-like**	**Source**	**Sequence ID**	**Translation?**	**Species Name**
He	FGFRL1	Levin et al., 2016 transcriptome	He_tr_04670	expasy	*Hypsibius exemplaris*
He	FGFRL2	Levin et al., 2016 transcriptome	He_tr_03639	expasy	*Hypsibius exemplaris*
Dm	Htl	UCSC	NP_732287		*Drosophila melanogaster*
Dm	Btl	UCSC	NP_729956		*Drosophila melanogaster*
Ce	Egl-15	UCSC	NP_001369987		*Caenorhabditis elegans*
Nv	FGFRa	GenBank	XP_048584433.1		*Nematostella vectensis*
Nv	FGFRb	GenBank	XP_048585038.1		*Nematostella vectensis*
Na	FGFR1	GenBank	QUP08111.1		*Novocrania anomala*
Tt	FGFR	GenBank	QUP08107.1		*Terebratalia transversa*
Ph	FGFR	GenBank	QUP08114.1		*Phoronopsis harmeri*
Hs	FGFR1	GenBank	AAH15035.1		*Homo sapiens*
Hs	FGFR2	GenBank	CAA96492.1		*Homo sapiens*

Hs	FGFR3	GenBank	XP_047305776.1		*Homo sapiens*
Hs	FGFR4	GenBank	NP_001341913.1		*Homo sapiens*
Bf	FGFR	GenBank	XP_035673320.1		*Branchiostoma floridae*
Species Abbrev.	**Non-FGFR RTKs**	**Source**	**Sequence ID**	**Translation?**	**Species Name**
He	VEGFR	Yanai	He_tr_02285	expasy	*Hypsibius exemplaris*
Dm	PVR	UCSC	NP_723365		*Drosophila melanogaster*
Ce	VER-1	UCSC	NP_497162		*Caenorhabditis elegans*
Ce	VER-3	UCSC	NP_509836		*Caenorhabditis elegans*
Ce	VER-4	UCSC	NP_509835		*Caenorhabditis elegans*
Hs	VGFR1	GenBank	NP_002010.2		*Homo sapiens*
Hs	VGFR2	GenBank	NP_002244.1		*Homo sapiens*
Hs	VGFR3	GenBank	NP_891555.2		*Homo sapiens*
Bf	VEGFR	GenBank	XP_035682136.1		*Branchiostoma floridae*
Species Abbrev.	**Snail**	**Source**	**Sequence ID**	**Translation?**	**Species Name**
He	Snail	Levin et al., 2016 transcriptome	Hduj_tr_05604	expasy	*Hypsibius exemplaris*
Dm	Snail	UCSC	NP_476732		*Drosophila melanogaster*
Dm	Escargot	UCSC	NP_476600		*Drosophila melanogaster*
Nv	SnaA	GenBank	AAR24456.1		*Nematostella vectensis*
Nv	SnaB	GenBank	AAR24457.1		*Nematostella vectensis*
Tc	Snail	GenBank	XP_971329.1		*Tribolium castaneum*
Hv	Snail	GenBank	XP_002162096.1		*Hydra vulgaris*
Ci	Snail	GenBank	AAB61226.1		*Ciona intestinalis*

Pf	Snail	GenBank	AXA20416.1		*Ptychodera flava*
Hs	SNAI1	GenBank	NP_005976.2		*Homo sapiens*
Bf	Snail	GenBank	AAC35351.1		*Branchiostoma floridae*
Species Abbrev.	**Scratch**	**Source**	**Sequence ID**	**Translation?**	**Species Name**
He	Scratch	Levin et al., 2016 transcriptome	Hduj_tr_06310	expasy	*Hypsibius exemplaris*
Dm	Scrt	UCSC	NP_523911.2		*Drosophila melanogaster*
Ce	CES-1	UCSC	NP_492338		*Caenorhabditis elegans*
Nv	Scratch2	GenBank	XP_032237161.1		*Nematostella vectensis*
Tc	Scratch1	GenBank	EFA13195.2		*Tribolium castaneum*
Tc	Scratch2	GenBank	EFA13196.1		*Tribolium castaneum*
Hs	Scratch1	GenBank	NP_112599.2		*Homo sapiens*
Hs	Scratch2	GenBank	NP_149120.1		*Homo sapiens*
Bf	Scratch1	GenBank	XP_035679385.1		*Branchiostoma floridae*
Bf	Scratch2	GenBank	XP_035679386.1		*Branchiostoma floridae*
Species Abbrev.	**Dpp/BMP2/4**	**Source**	**Sequence ID**	**Translation?**	**Species Name**
He	Dpp	Levin et al., 2016 transcriptome	He_tr_08636	expasy	*Hypsibius exemplaris*
Dm	Dpp	UCSC	NP_477311		*Drosophila melanogaster*
Dm	Scw	UCSC	NP_524863		*Drosophila melanogaster*
Mm	BMP2	GenBank	NP_031579.2		*Mus musculus*
Mm	BMP4	GenBank	NP_001303289.1		*Mus musculus*
Nv	BMP2/4	GenBank	AAR13362.1		*Nematostella vectensis*
Tc	Dpp	GenBank	NP_001034540.1		*Tribolium*

					castaneum
Species Abbrev.	**Gbb/BMP5/7/8**	**Source**	**Sequence ID**	**Translation?**	**Species Name**
He	Gbb	Levin et al., 2016 transcriptome	He_tr_00999	expasy	*Hypsibius exemplaris*
Dm	Gbb	UCSC	NP_477340		*Drosophila melanogaster*
Mm	BMP5	GenBank	NP_031581.2		*Mus musculus*
Mm	BMP7	GenBank	NP_031583.2		*Mus musculus*
Mm	BMP8B	GenBank	NP_031585.2		*Mus musculus*
Mm	BMP8A	GenBank	NP_031584.1		*Mus musculus*
Nv	BMP5/7/8	GenBank	XP_032219054.1		*Nematostella vectensis*
Tc	Gbb	GenBank	NP_001107813.1		*Tribolium castaneum*
Species Abbrev.	**Other BMPs**	**Source**	**Sequence ID**	**Translation?**	**Species Name**
Mm	BMP3	GenBank	NP_775580.1		*Mus musculus*
Mm	BMP6	GenBank	NP_031582.1		*Mus musculus*
Mm	BMP9/GDF2	GenBank	NP_062379.3		*Mus musculus*
Mm	BMP10	GenBank	NP_033886.2		*Mus musculus*
Species Abbrev.	**Sog/Chordin**	**Source**	**Sequence ID**	**Translation?**	**Species Name**
He	sog	Levin et al., 2016 transcriptome	He_tr_06660	expasy	*Hypsibius exemplaris*
Dm	sog	UCSC	NP_001259578		*Drosophila melanogaster*
Mm	chordin	NCBI_GenBank	AAD19895.1		*Mus musculus*
Xl	chordin	NCBI_GenBank	AAC42222.1		*Xenopus laevis*
Tc	sog	NCBI_GenBank	ABF22614.1		*Tribolium castaneum*
Am	sog	NCBI_GenBank	XP_006570089.1		*Apis mellifera*
Hs	chordin	NCBI_GenBank	AAG35767.1		*Homo sapiens*

Ci	chordin	NCBI_GenBank	XP_026690585.1		*Ciona intestinalis*
Nv	chordin	NCBI_GenBank	ABC88373.1		*Nematostella vectensis*
Species Abbrev.	**Tkv/Type I receptor**	**Source**	**Sequence ID**	**Translation?**	**Species Name**
He	Tkv	Levin et al., 2016 transcriptome	He_tr_10719	expasy	*Hypsibius exemplaris*
Dm	Tkv	UCSC	NP_787989		*Drosophila melanogaster*
Gb	Tkv	NCBI_GenBank	AHJ59839.1		*Gryllus bimaculatus*
Tc	Tkv	NCBI_GenBank	EFA09250.1		*Tribolium castaneum*
Mm	BMPR1a	NCBI_GenBank	XP_036014306.1		*Mus musculus*
Nv	BMPR1b	NCBI_GenBank	XP_001633896.2		*Nematostella vectensis*
Species Abbrev.	**Punt/Type II receptor**	**Source**	**Sequence ID**	**Translation?**	**Species Name**
He	Punt	Levin et al., 2016 transcriptome	He_tr_12285	expasy	*Hypsibius exemplaris*
Dm	Punt	UCSC	NP_001262574		*Drosophila melanogaster*
Tc	Punt	NCBI_GenBank	EEZ97734.1		*Tribolium castaneum*
Mm	BMPR2	NCBI_GenBank	EDL00137.1		*Mus musculus*
Nv	BMPR2	NCBI_GenBank	XP_048588435.1		*Nematostella vectensis*
Species Abbrev.	**Sax/Type II receptor**	**Source**	**Sequence ID**	**Translation?**	**Species Name**
He	Sax	Levin et al., 2016 transcriptome	He_tr_01951	expasy	*Hypsibius exemplaris*
He	Babo	Levin et al., 2016 transcriptome	He_tr_12110	expasy	*Hypsibius exemplaris*
Dm	Sax	UCSC	NP_523652		*Drosophila melanogaster*

Dm	Babo	UCSC	NP_477000		*Drosophila melanogaster*
Tc	Babo	NCBI_GenBank	KYB28937.1		*Tribolium castaneum*
Tc	Sax	NCBI_GenBank	CDW20669.1		*Tribolium castaneum*
Dm	Wit	NP_524692	UCSC		*Drosophila melanogaster*
Tc	Wit	EFA07475.1	NCBI_GenBank		*Tribolium castaneum*
Species Abbrev.	**Tld**	**Source**	**Sequence ID**	**Translation?**	**Species Name**
He	Tld	Levin et al., 2016 transcriptome	Hduj_tr_05721	expasy	*Hypsibius exemplaris*
Dm	Tld	UCSC	NP_524487		*Drosophila melanogaster*
Dr	Tld	NCBI_GenBank	AAC60304.1		*Danio rerio*
Gg	Tld	NCBI_GenBank	NP_990034.2		*Gallus gallus*
Tc	Tld	NCBI_GenBank	KYB28517.1		*Tribolium castaneum*
Am	Tld	NCBI_GenBank	XP_006567026.2		*Apis mellifera*
Hs	Tld	NCBI_GenBank	KAI4027581.1		*Homo sapiens*
Ci	Tld	NCBI_GenBank	NP_001071840.1		*Ciona intestinalis*
Nv	Tld	NCBI_GenBank	XP_001633846.2		*Nematostella vectensis*
Species Abbrev.	**Doc1**	**Source**	**Sequence ID**	**Translation?**	**Species Name**
He	Doc1	Levin et al., 2016 transcriptome	HD_v1_tr_01406	expasy	*Hypsibius exemplaris*
Dm	Doc1	UCSC	NP_648283		*Drosophila melanogaster*
Tc	Doc	NCBI_GenBank	EFA10735.1		*Tribolium castaneum*
Mm	Tbx6	NCBI_GenBank	AAT72924.1		*Mus musculus*
Xl	Tbx6	NCBI_GenBank	ABC75836.1		*Xenopus laevis*
Xl	VegT	NCBI_GenBank	AAB93301.1		*Xenopus laevis*

Mm	Brachyury	NCBI_GenBank	AAI20808.1		*Mus musculus*
Mm	Tbx2	NCBI_GenBank	AAC52697.1		*Mus musculus*
Mm	Tbx20	NCBI_GenBank	NP_919239.1		*Mus musculus*
He	Omb	Levin et al., 2016 transcriptome	Hduj_tr_06618	expasy	*Hypsibius exemplaris*
Dm	Omb	UCSC	NP_525070		*Drosophila melanogaster*
Species Abbrev.	**Eya**	**Source**	**Sequence ID**	**Translation?**	**Species Name**
He	Eya	Levin et al., 2016 transcriptome	HD_v1_tr_10204	expasy	*Hypsibius exemplaris*
Dm	Eya	UCSC	NP_723188		*Drosophila melanogaster*
Ce	Eya-1	UCSC	NP_001367120		*Caenorhabditis elegans*
Mm	Eya1	NCBI_GenBank	NP_001297388.1		*Mus musculus*
Dr	Eya1	NCBI_GenBank	AAI54188.1		*Danio rerio*
Hs	Eya1	NCBI_GenBank	AAI21799.1		*Homo sapiens*
Nv	Eya	NCBI_GenBank	XP_032233587.1		*Nematostella vectensis*
At	Eya	NCBI_GenBank	NP_565803.1		*Arabidopsis thaliana*

Table 2 Primers used for cloning

Primers		
Target	**Direction**	**Sequence (5’ → 3’)**
dpp	F1	acctgacgagcgtacattcc
	R1	aactgctccagccaatctcc
	F2	ccgcttctaacggctcatcc
	R2	ccccggcgatacttcttcac
gbb	F1	acggcatcgaccaatccatc
	R1	gtaggccgagtaaccatccg
	F2	atcgaccaatccatcccgc
	R2	gaagaacgccaccatgaagc
sog	F1	agcagcagcagtatcgtttg
	R1	tccgtcgagaatccttagcc
	F2	cagcagcagtatcgtttgtttg
	R2	taatggtccccttgtagccg
tkv	F1	tccttcatcttttgcgtggc
	R1	ctctggggtggtagtcagtg
	F2	aacagtaaatgcttcgccgc
	R2	ccaagaaggttgtcgtgtcg
punt	F1	ctatggggaggtgtggaagg
	R1	catgcgattgagcagacagg
	F2	tatggggaggtgtggaaggg
	R2	agggtttgaaggaaggtcgg
fgf8	F1	taatcgtcttccttgcagcc
	R1	tagaggagggtcttcagcg
	F2	gcagcctcatcccttcttc
	R2	ccggtggaagttgtagcag
fgfrl1	F1	agcggaatttacaactgcac
	R1	aactttgggtgttttgacgg
	F2	atatcatggggtcgcatcc
	R2	caatggttcgttcctccttg

fgfrl2	F1	acggactctcacaatcagac
	R1	caagagcagcaacatgactc
	F2	catccttcatccaactgggg
	R2	ggcaatgtttttctgcattcg
snail	F1	cctcccatactttccgtctc
	R1	tcaggcatatcaggcacttg
	F2	caacaacttctcaccgttcc
	R2	agattttgcagtcgtaaggc
tld	F1	agacccttcttatgcccaac
	R1	atacagctctggaaaggacg
	F2	agcaaagagtgccagttagg
	R2	aaagatggtcccgttcaagg
doc1	F1	gatacactccagtctcctgc
	R1	tgaacaaaacgggaacatgg
	F2	tctcctgccaatcatgtacc
	R2	aaggtctcggaagcctttag
eya	F1	acaatatggagcgcgttttc
	R1	caggtgatcattctccaggg
	F2	atagacccacattcgacacg
	R2	ctgcaggttaagcagttgtg

Table 3 Some hypotheses of FGF and BMP Functions

Pathway(s)	Relevant Pattern	Hypothesis
FGF	*fgf8* patches form dynamically over time during endomesodermal segmentation	Another gene (possibly Ets4) induces *fgf8* patch formation
	fgf8 patches increase in number and decrease in size	Patches arise from independent cell populations
	fgf8 patches change orientation relative to embryo axes	The same cells expressing *fgf8* tangential to the A-P axis then move to be perpendicular to the A-P axis
	fgf8 patches occur adjacent to the ectodermal furrow sites	patches regulate ectodermal furrow formation
	fgf8 patches occur in the layer above endomesodermal pouches	FGF8 guides migration of underlying mesoderm
	fgf8 patches occur in layer above endomesodermal pouches	FGF8 patterns muscle-body wall attachment sites
	fgf8 patches occur in layer above endomesodermal pouches	FGF8 regulates fate commitment of mesodermal cells
	fgf8 patches occur in layer above endomesodermal pouches and change orientation with respect to body axes during ectodermal segmentation	*fgfrl1*-expressing endomesoderm feeds back on *fgf8*-expressing ectoderm to regulate ectodermal segmentation
	fgf8 expressed in band at posterior of head segment	FGF8 regulates regionalization of the unipartite brain
	fgf8 expressed in a posterior region of the developing foregut	FGF8 regulates formation of the esophagus in the foregut
	fgf8 patches occur in the posterior of body segments	FGF8 provides posterior cues along the A-P axis of body segments
	fgf8 patches occur in layer above endomesodermal pouches; *eya* is enriched in endomesoderm	FGF8 regulates *eya* expression
BMP	*dpp* extends more dorsally than *sog* laterally along the embryo	Dpp regulates D-V patterning
	dpp extends more dorsally than *sog* laterally along the embryo	Dpp informs D-V position of future limbs
	dpp extends more dorsally than *sog* laterally along the embryo	Sog prevents limbs from forming too far ventrally or in internal cells
	dpp extends more dorsally than *sog* laterally along the embryo	Dpp regulates cuticle deposition and patterning
	sog bands on either side of developing mouth; *dpp* beyond and overlapping *sog* bands	Dpp regulates mouth formation and Sog limits or concentrates the functional domain of Dpp
	dpp is expressed in ectoderm above	Dpp regulates mesoderm development

	endomesoderm	
	dpp is expressed laterally along the body	Dpp regulates development and/or positioning of neural trunk ganglia
	gbb is enriched in most cells except PGCs; *tkv* and *punt* are enriched in most cells including the PGCs	Gbb regulates PGC fate acquisition, maintenance, and/or development
	sog bands on either side of developing mouth; *dpp* beyond and overlapping *sog* bands; *tld* stretches between *sog* bands	Tld facilitates spreading of Dpp (with Sog) to the developing mouth or to the anterior endomesodermal pouches
	tld expressed across developing mouth	Tld regulates pharyngeal development through control of ECM independent of Dpp
	snail expressed in ectoderm and endomesoderm	non-mesodermal cells express snail early and later snail expression is restricted to mesoderm
	snail expressed in ectoderm and endomesoderm	neuroectoderm cells express *snail*
	doc1 enriched in dorsal stripe; *dpp* extends more dorsally than *sog* laterally along the embryo	Dpp regulates *doc1* expression along dorsal ridge of embryo
	dpp is expressed in ectoderm above endomesoderm; *eya* enriched in endomesoderm	Dpp regulates *eya* expression
	gbb is enriched in most cells except PGCs; *tkv* and *punt* are enriched in most cells including the PGCs; *eya* is expressed in PGCs	Gbb regulates *eya* expression in PGCs and/or the entire embryo
BMP+FGF	*fgf8* and *dpp* enriched in ectoderm	Fgf8 and Dpp work together to regulate proper mesoderm formation and/or fate

Figure 1

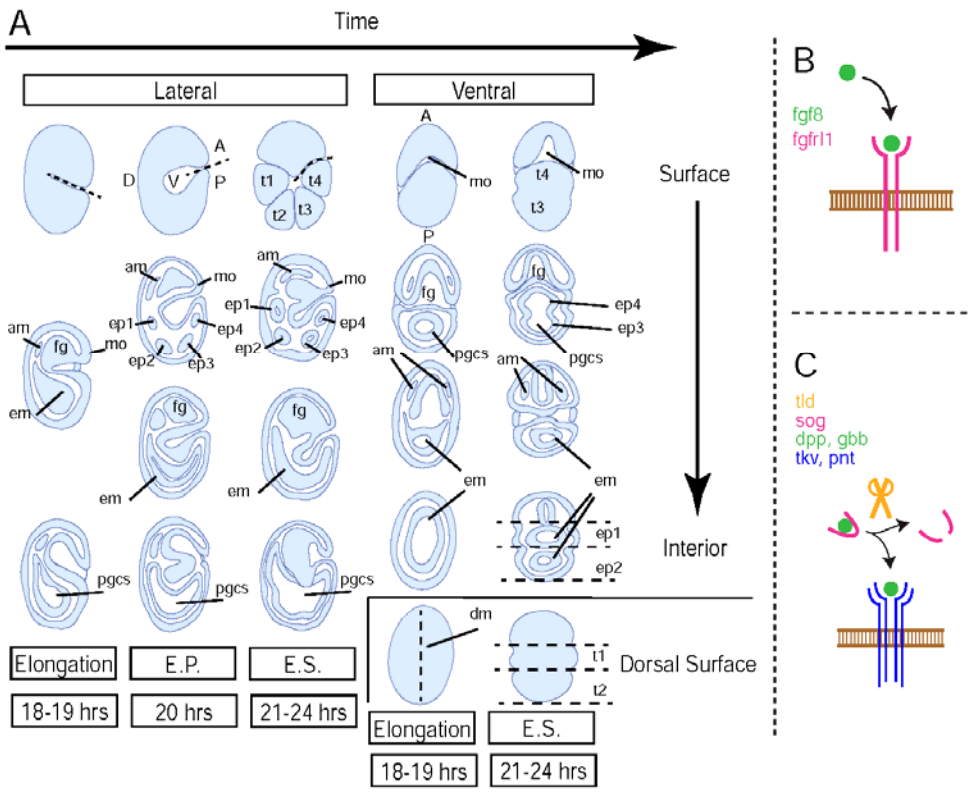

Figure 1 Introduction to morphology of *Hypsibius exemplaris* embryos between elongation and segmentation stages.

A. Drawings representative of *H. exemplaris* embryos at elongation, endomesodermal pouch formation (E.P.), and ectodermal segmentation (E.S.) stages, shown from right lateral and ventral views. From top to bottom, images show surface to internal views (and dorsal surface for ventral views). Anterior (A) is up and Posterior (P) is down in all drawings. Dorsal (D) and (V) are to the left and right, respectively, in the lateral views. Certain morphological features are labelled: mouth (mo), anterior mesoderm (am), dorsal midline (dm), foregut (fg), endomesoderm (em), endomesodermal pouch (ep), trunk segment (t), and primordial germ cells (pgcs). B. Schematic of FGF signaling showing extracellular ligand (green) binding transmembrane receptors (magenta), which dimerize. C. Schematic of BMP signaling showing extracellular ligand (green) binding extracellular antagonist (magenta), which is cleaved by extracellular protease (orange), free the ligand to bind transmembrane receptors (blue), which form a heterotetramer.

Figure 2

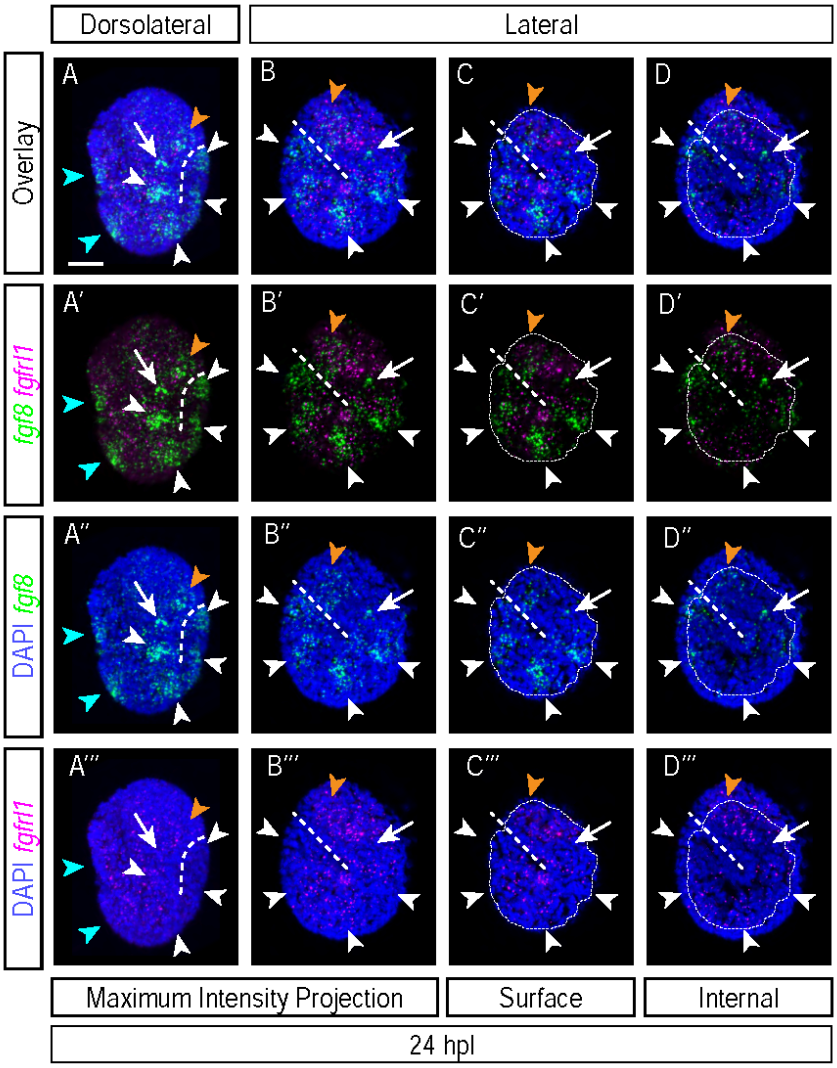

Figure 2 Expression patterns of *fgf8* and *fgfrl1* mRNAs at 24 hpl reveal ectodermal patches of *fgf8* in segment posteriors and global expression and endomesodermal enrichment of *fgfrl1*.

A-D. Expression patterns of *fgf8* and *fgfrl1* at 24 hpl (n=5 experiments, 8, 3, 4, 2, and 2 embryos respectively). A-B. Maximum intensity projections of embryos from a dorsolateral (A) and lateral (B) view. C. Projection of uppermost layers of the embryo in B. D. Projection of internal layers of the embryo in B. Small region outlined with a dashed line indicates the upper layers projected in C, which are omitted in the internal layers projected in D. Arrowheads indicate ectodermal patches of *fgf8* signal in trunk segment posteriors. Blue arrowheads indicate two of the ectodermal patches of *fgf8* signal running along the left side of the embryo in A. Orange arrowheads indicate the anterior head segment patch of *fgf8* signal. Arrows indicate small groups of ectodermal and endomesodermal cells enriched for *fgf8* at the posterior of head segments. Right dorsolateral view in A. Left lateral view in B-D. Scale bar = 10 μm.

Figure 3

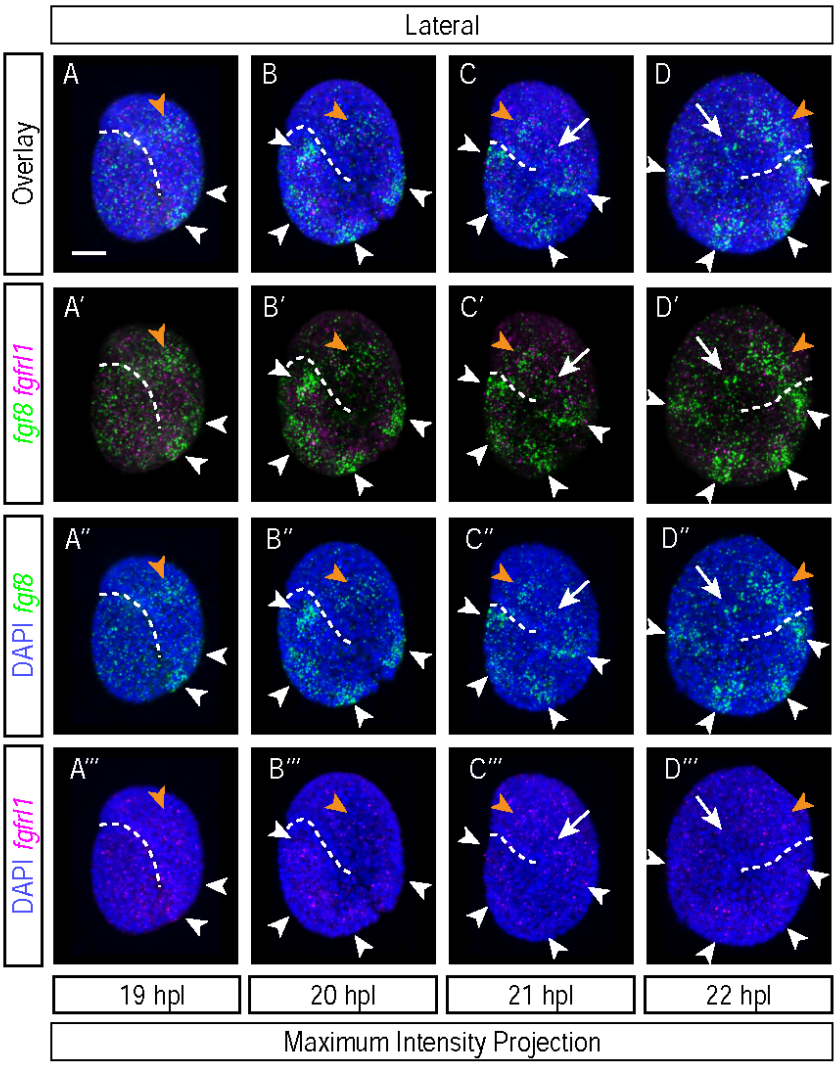

Figure 3 Lateral ectoderm patches of *fgf8* mRNA arise prior to ectodermal segmentation and near the time of endomesodermal pouch formation.

A-D. Expression patterns of *fgf8* and *fgfrl1* mRNAs at 19 hpl (A, n=2 experiments, 8 and 4 embryos) 20 hpl (B, n=3 experiments, 9, 8, and 6 embryos) 21 hpl (C, n=5 experiments, 8, 11, 6, 5, and 7 embryos) and 22 hpl (D, n=5 experiments, 8, 3, 4, 2, and 2 embryos). All images are maximum intensity projections of embryo from lateral views. Arrowheads indicate ectodermal patches of *fgf8* signal. Orange arrowheads indicate the patch of *fgf8* signal in the anterior of head segments. Arrows indicate small groups of cells enriched for *fgf8* at the posterior of head segments. Left lateral view in A-C. Right lateral view in D. Scale bar = 10 µm.

Figure 4

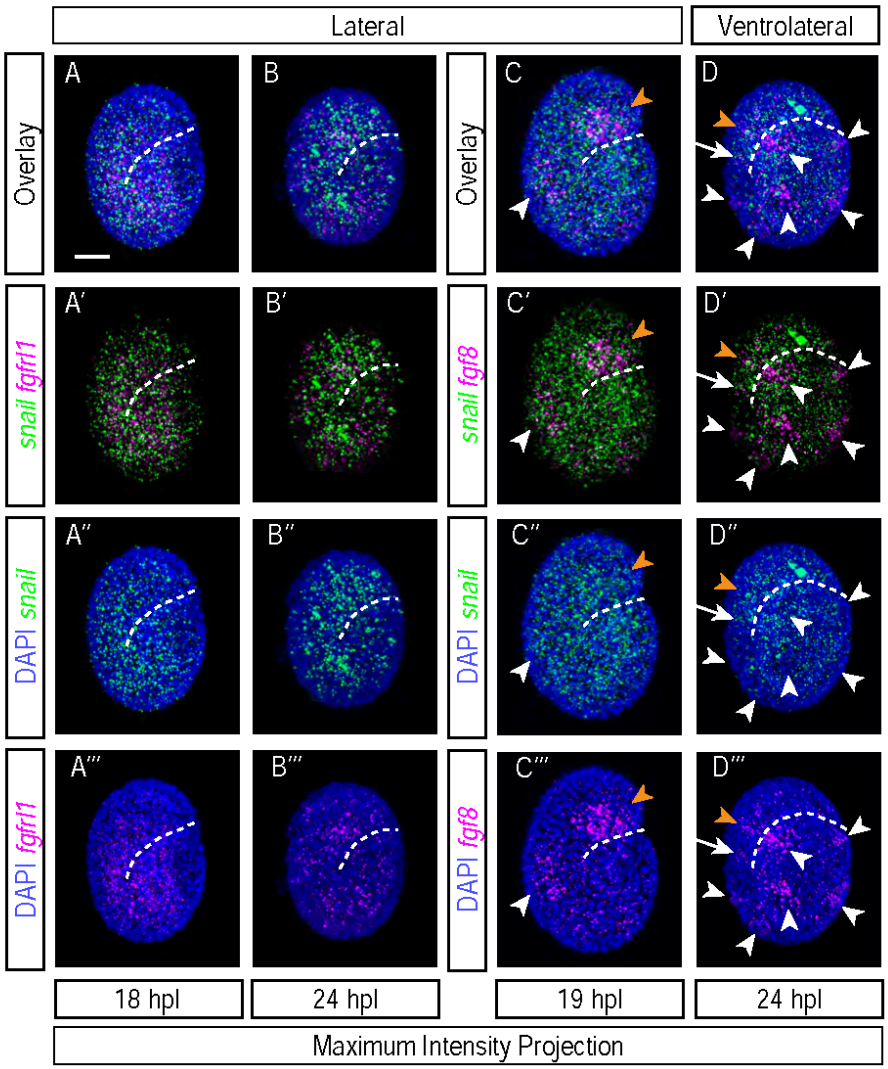

Figure 4 mRNA of the mesodermal transcription factor *snail* is present in non-mesodermal cells.

A-B. Enrichment patterns of *snail* and *fgfrl1* mRNAs at 18 hpl (A, n=2 experiments, 8 and 2 embryos) and 24 hpl (B, n=2 experiments, 1 and 3 embryos). C-D. Enrichment patterns of *snail* and *fgf8* mRNAs at 19 hpl (C, n=2 experiments, 8 and 6 embryos) and 24 hpl (D, n=2 experiments, 8 and 5 embryos). All images are maximum intensity projections. Arrowheads indicate ectodermal patches of *fgf8* signal. Orange arrowheads indicate the patch of *fgf8* signal in the anterior of head segments. Arrows indicate small groups of cells enriched for *fgf8* at the posterior of head segments. Right lateral view in A-C. Right ventrolateral view in D. Scale bar = 10 µm.

Figure 5

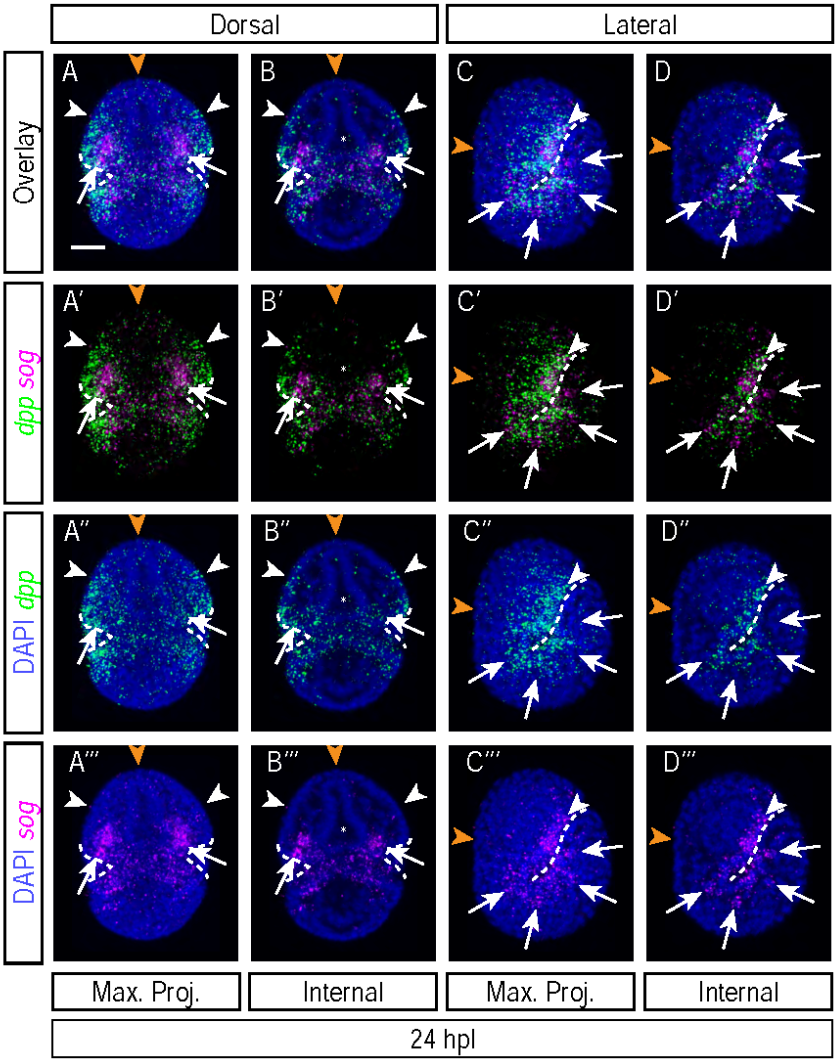

Figure 5 mRNAs of BMP ligand *dpp* and antagonist *sog* are expressed in lateral ectoderm, with *dpp* expressed more dorsally than *sog.*

A-D. Enrichment patterns of *dpp* and *sog* mRNAs at 24 hpl (n=6 experiments, 6, 1, 1, 1, 2, and 13 embryos). A and C Maximum intensity projections of embryos from a dorsal (A) and lateral (C) view. B. Projection of internal layers of the embryo in A. D. Projection of internal layers of the embryo in C. Arrowheads indicate the extent of spread of *dpp* mRNA dorsally. Orange arrowheads indicate the absence of enrichment for *dpp* and *sog* at the dorsal midline of the embryo. Arrows in A-B indicate bands of cells enriched for *sog* on either side of the developing mouth. Arrows in C-D indicate the endomesodermal cells enriched for *sog* in each endomesodermal pouch. Asterisks in A-B indicate the hollow space within the developing foregut, which is not enriched for *sog* in its epithelium. Dorsal view in A and B. Right lateral view in C and D. Scale bar = 10 µm.

Figure 6

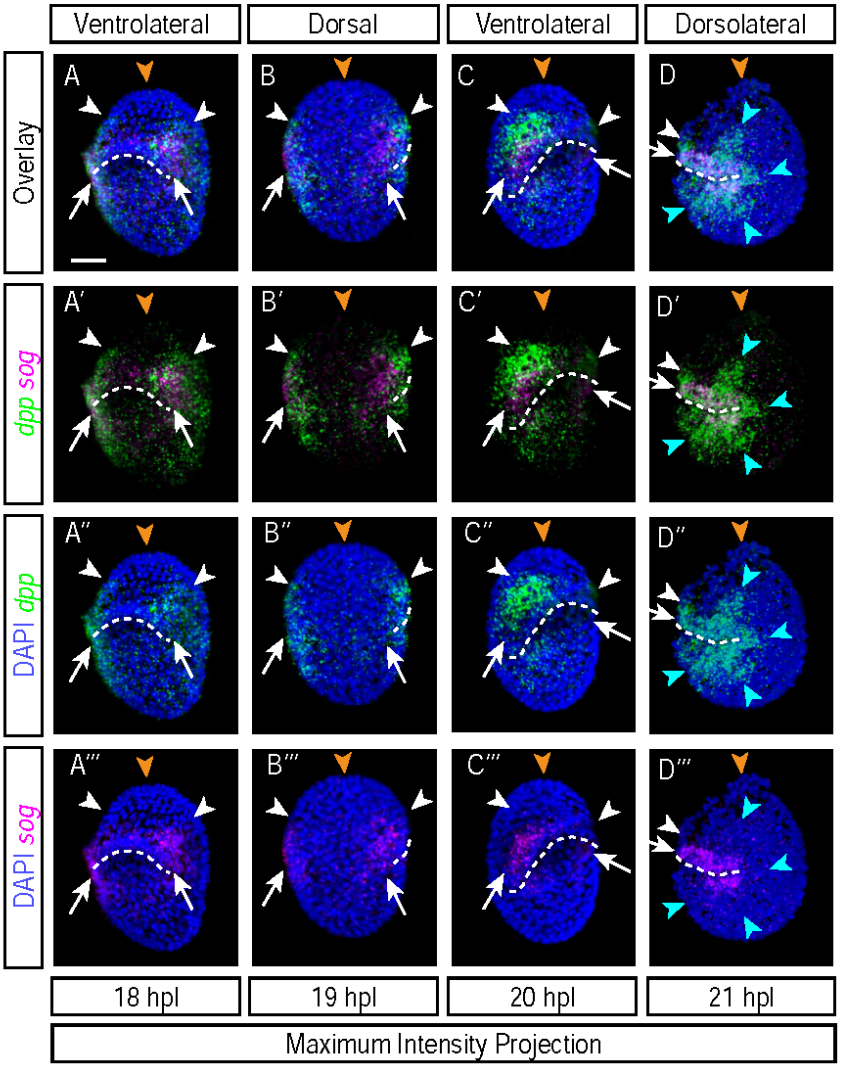

Figure 6 Expression of *dpp* and *sog* mRNAs changes between elongation and segmentation.

A-D. Enrichment patterns of *dpp* and *sog* mRNAs at 18 hpl (A, n=3 experiments, 13, 2, and 1 embryos) 19 hpl (B, n=1 experiment, 7 embryos) 20 hpl (C, n=1 experiment, 7 embryos), and 21 hpl (D, n=3 experiments, 10, 16, and 2 embryos). All images are maximum intensity projections. Arrowheads indicate the extent *dpp* mRNA expression dorsally. Orange arrowheads indicate the absence of enrichment for *dpp* and *sog* at the dorsal midline. Arrows indicate bands of cells enriched for *sog* on either side of the developing mouth. Blue arrowheads indicate bands of *dpp* running over each segment. Left ventrolateral view in A. Dorsal view in B. Right ventrolateral view in C. Left dorsolateral view in D. Scale bar = 10 µm.

Figure 7

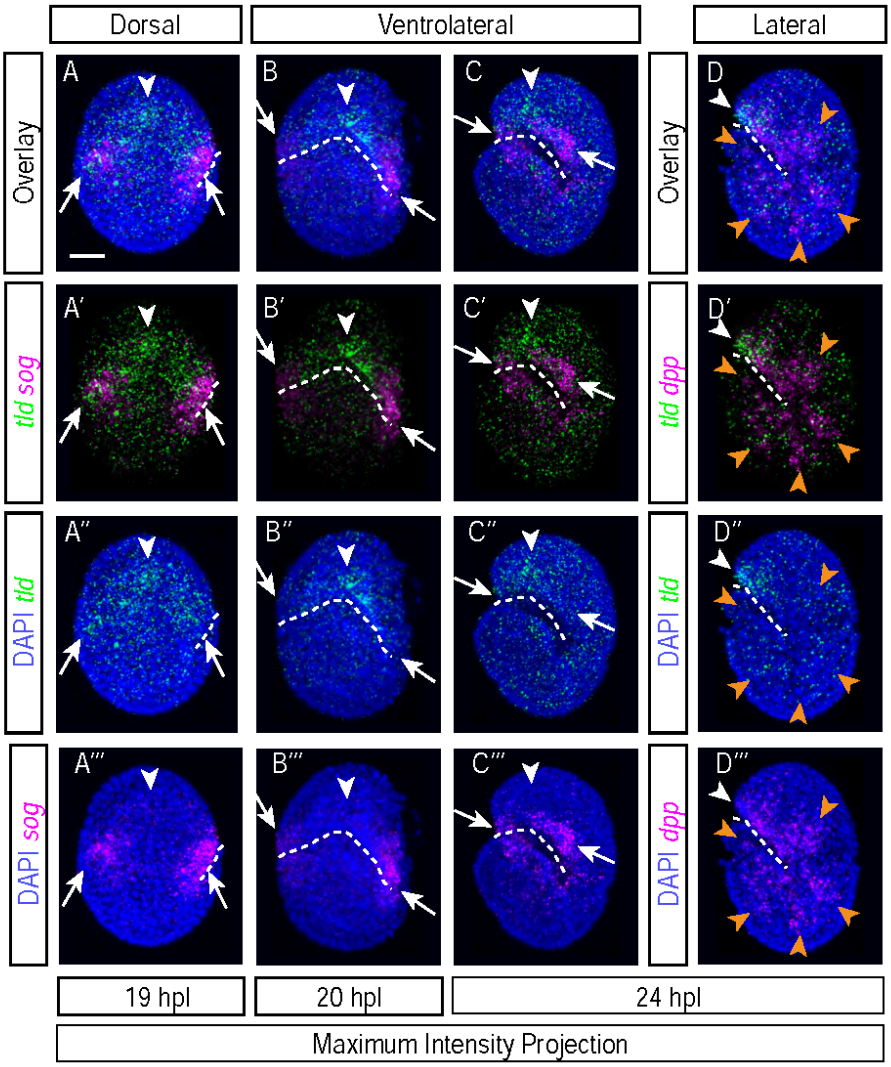

Figure 7 mRNAs of protease tld become more restricted along the anterior-most ridge of the head from 19 to 24 hpl.

A-C. Enrichment patterns of *tld* and *sog* mRNAs at 19 hpl (A, n=1 experiment, 6 embryos), 20 hpl (B, n=1 experiment, 7 embryos), and 24 hpl (C, n=4 experiments, 5, 7, 2, and 2 embryos). D. Enrichment patterns of *tld* and *dpp* mRNAs at 24 hpl (n=5 experiments, 13, 2, 1, 2, and 3 embryos). All images are maximum intensity projections. Arrowheads indicate the band of *tld* along the anterior ridge of the embryo. Arrows indicate bands of cells enriched for *sog* on either side of the developing mouth. Orange arrowheads indicate the bands of *dpp* running over each segment. Dorsal view in A. Left ventrolateral view in B-C. Left lateral view in D. Scale bar = 10 µm.

Figure 8

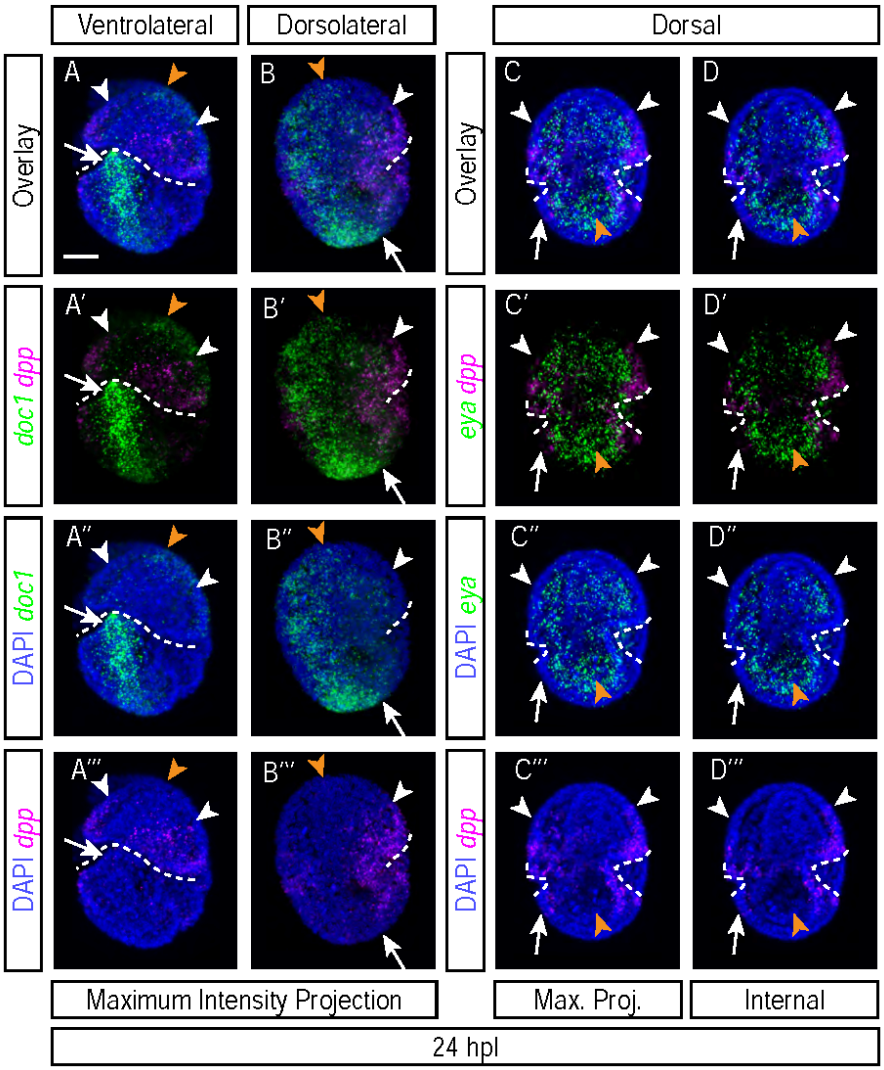

Figure 8 Expression patterns of *doc1, eya,* and *dpp* at ectodermal segmentation stage (24 hpl).

A-B. Enrichment patterns of *doc1* and *dpp* mRNAs at 24 hpl (n=4 experiments, 10, 1, 5, and 2 embryos). C-D. Enrichment patterns of *eya* and *dpp* mRNAs at 24 hpl (n=2 experiments, 9 and 2 embryos). A-C. Maximum intensity projections of embryos. D. Projection of internal layers of the embryo in C. Arrowheads in A-D indicate the extend of spread of *dpp* mRNA dorsally. Orange arrowheads in A-B indicate the anterior end of the band of *doc1* along the dorsal midline. Arrows in A-B indicate the posterior end of the band of *doc1* along the dorsal midline. Arrows in C-D indicate the ectodermal layer, which is not enriched for *eya*. Orange arrowheads in C-D indicate the region of the PGCs, which is enriched for *eya*. Left ventrolateral view in A. Right dorsolateral view in B. Dorsal view in C-D. Scale bar = 10 µm.

Figure 9

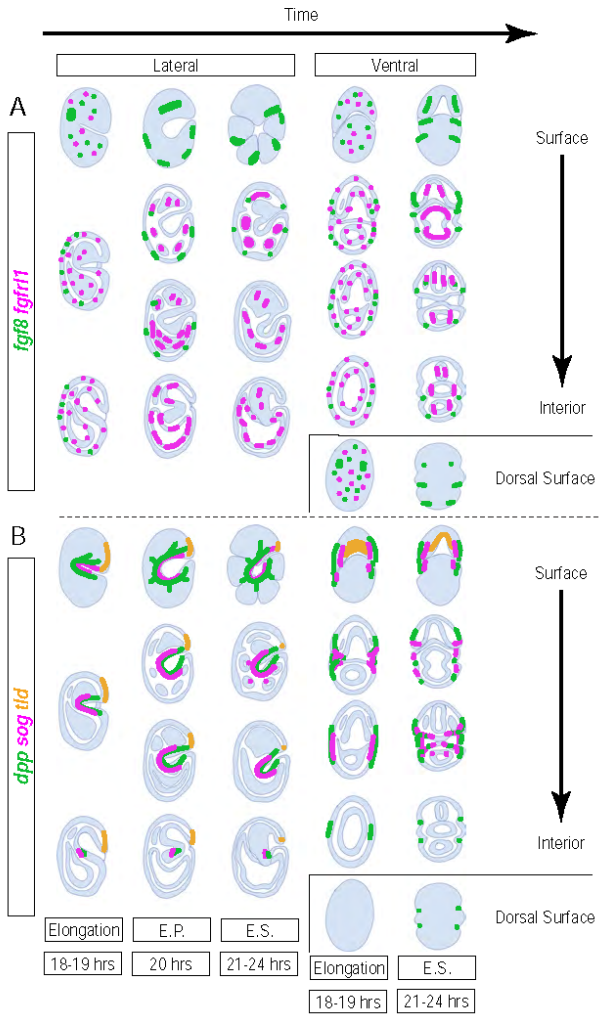

Figure 9 Summary of BMP and FGF pathway gene patterns of enrichment in *H. exemplaris* embryos between elongation and segmentation stages.

Drawings representative of enrichment patterns of (A) FGF and (B) BMP signaling pathway genes in *H. exemplaris* embryos at elongation, endomesodermal pouch formation (E.P.), and ectodermal segmentation (E.S.) stages, shown from lateral and ventral views. From top to bottom, images show surface to internal views (and dorsal surface below ventral views). Anterior (A) is up and Posterior (P) is down in all drawings. Dorsal (D) and (V) are to the left and right, respectively, in the lateral views. Representative summaries of expression patterns are shown as follows: in the top embryos (A), *fgf8* in green, *fgfrl1* in magenta; in the bottom embryos (B), *dpp* in green, *sog* in magenta, *tld* in orange.

Supplementary Figure 1

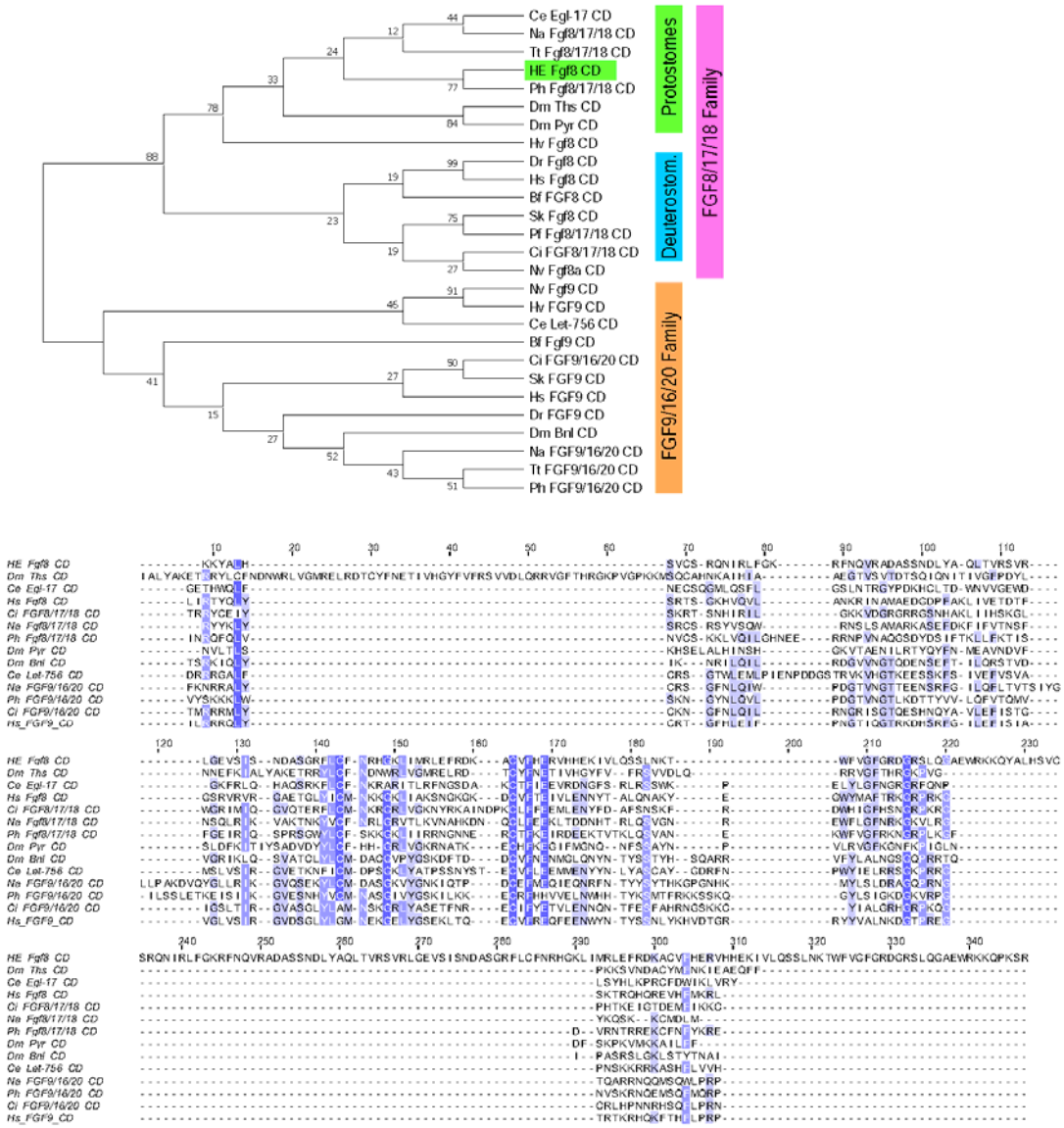

Supplementary Figure 1 Identification of an FGF8 homolog in *H. exemplaris*

Above: Maximum Likelihood phylogenetic reconstruction of FGF8 and related amino acid sequences. Branch support out of 100 is given at each node. *H. exemplaris* sequences are highlighted. Protein families are indicated by colored bars to the right of the tree. Deuterostom = Deuterostomes. Below: Alignment used for phylogenetic reconstruction from conserved domain among FGF homologs from several species. Genes include 2-letter prefixes indicating species listed in Table 1.

Supplementary Figure 2

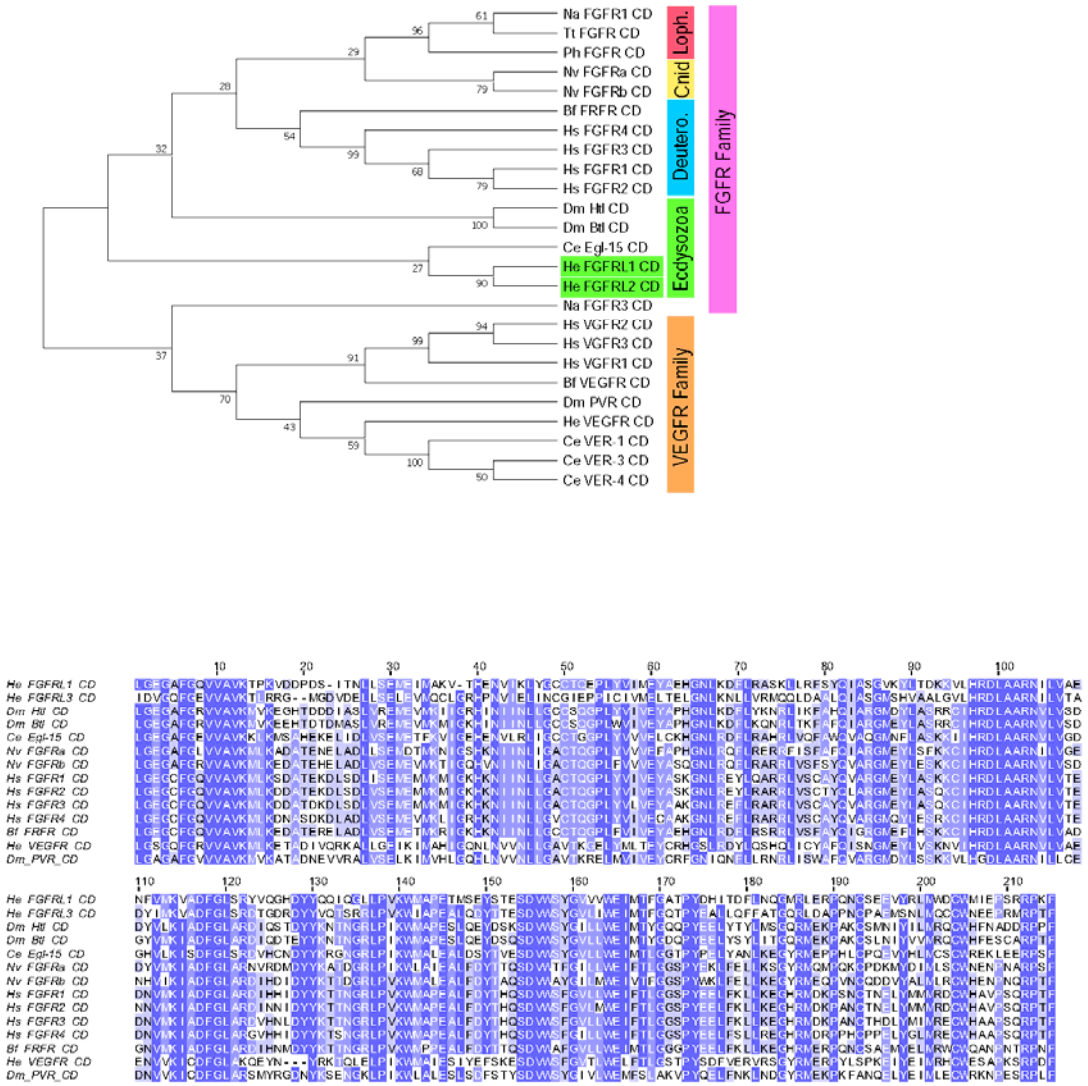

Supplementary Figure 2 Identification of FGF Receptor homologs in *H. exemplaris*

Above: Maximum Likelihood phylogenetic reconstruction of FGF receptors and related amino acid sequences. Branch support out of 100 is given at each node. *H. exemplaris* sequences are highlighted. Protein families are indicated by colored bars to the right of the tree. Cnid = Cnidaria; Loph. = Lophotrocozoa; Deutero = Deuterostomes. Below: Alignment used for phylogenetic reconstruction from conserved domain among FGF receptor homologs from several species. Genes include 2-letter prefixes indicating species listed in Table 1.

Supplementary Figure 3

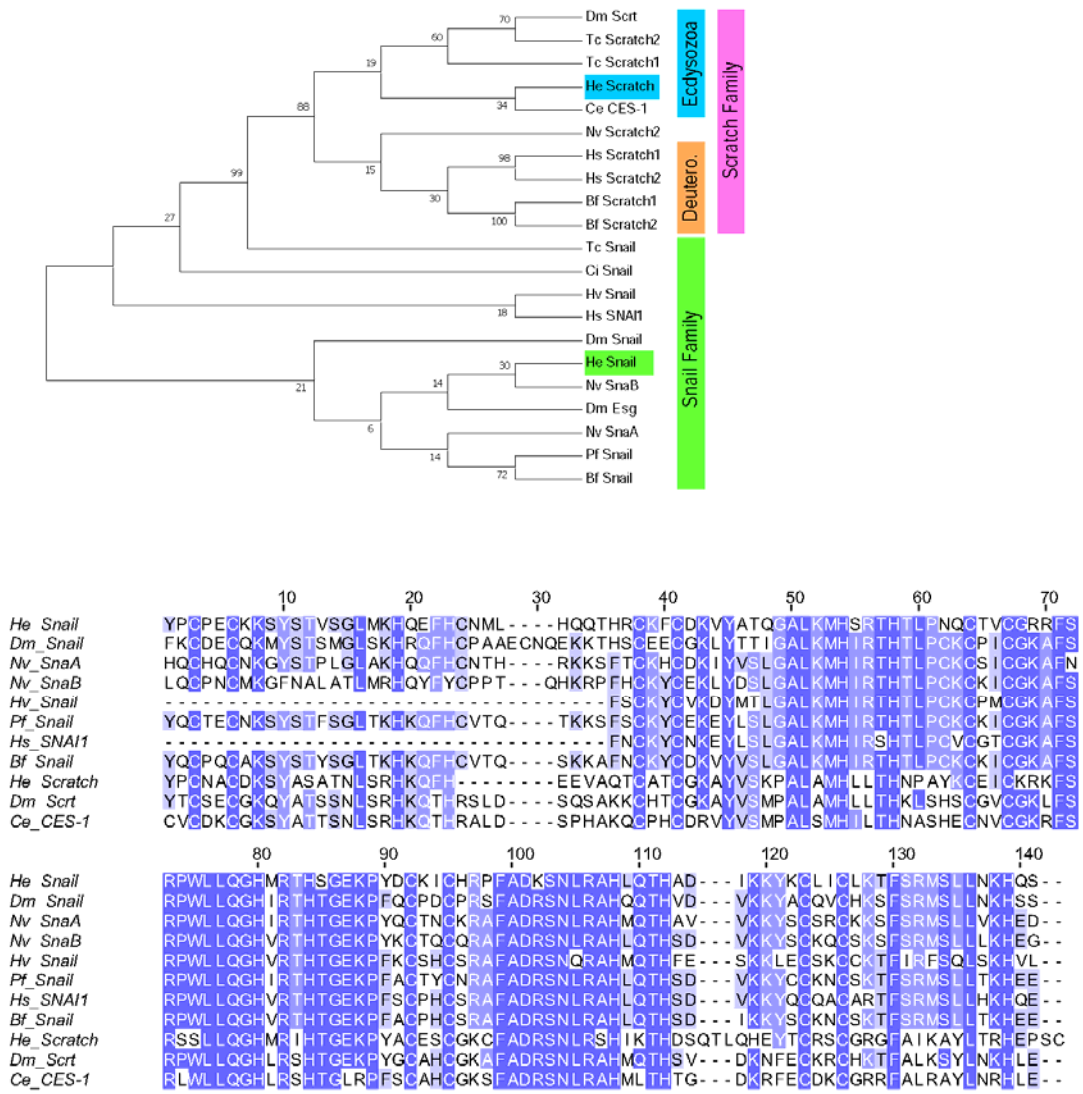

Supplementary Figure 3 Identification of a Snail homolog in *H. exemplaris*

Above: Maximum Likelihood phylogenetic reconstruction of Snail and related amino acid sequences. Branch support out of 100 is given at each node. *H. exemplaris* sequences are highlighted. Protein families are indicated by colored bars to the right of the tree. Deutero = Deuterostomes. Below: Alignment used for phylogenetic reconstruction from conserved region among Snail homologs from several species. Genes include 2-letter prefixes indicating species listed in Table 1.

Supplementary Figure 4

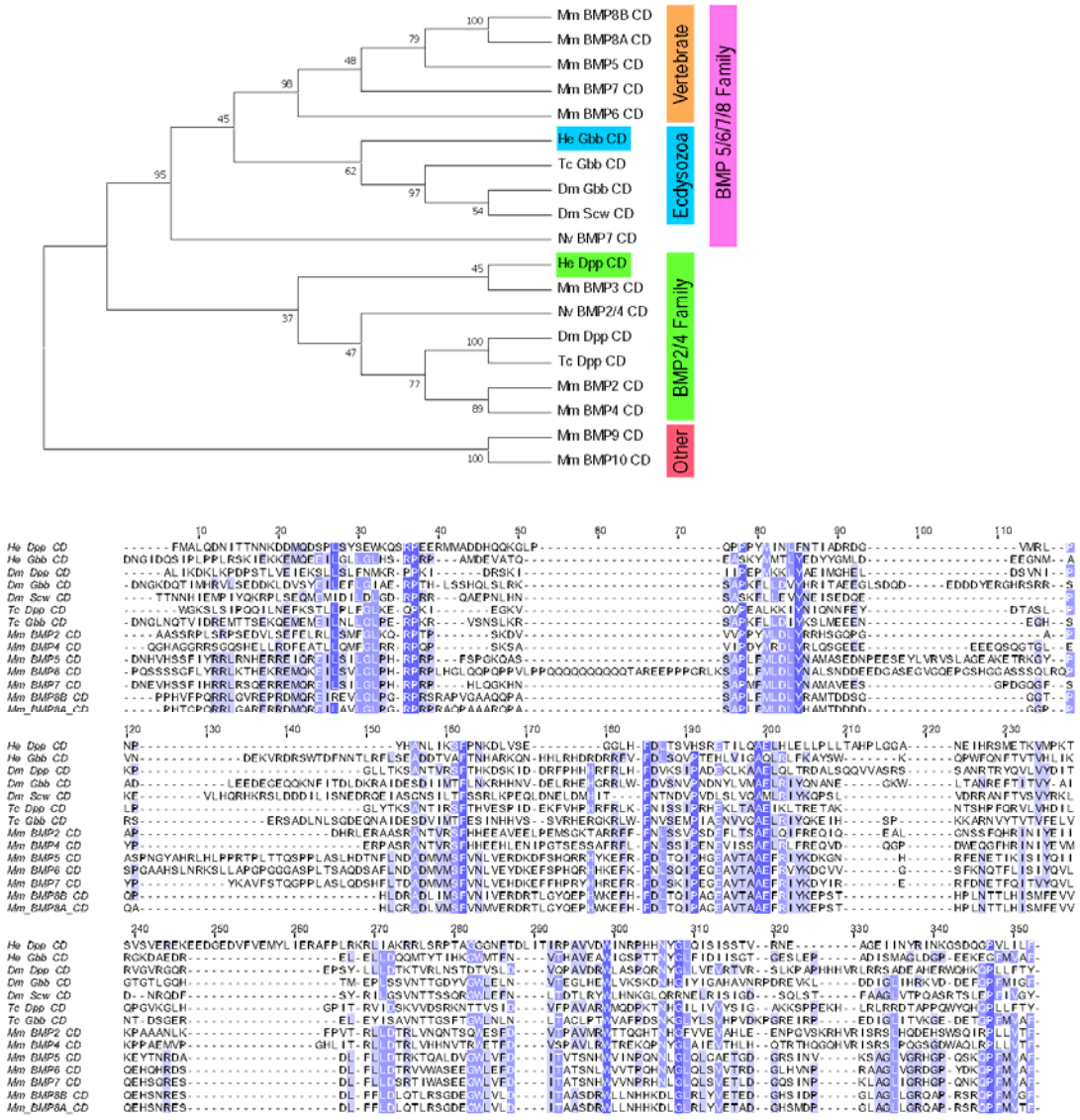

Supplementary Figure 4 Identification of BMP ligand homologs in *H. exemplaris*

Above: Maximum Likelihood phylogenetic reconstruction of BMP ligands and related amino acid sequences. Branch support out of 100 is given at each node. *H. exemplaris* sequences are highlighted. Protein families are indicated by colored bars to the right of the tree. Below: Alignment used for phylogenetic reconstruction from conserved domain among BMP homologs from several species. Genes include 2-letter prefixes indicating species listed in Table 1.

Supplementary Figure 5

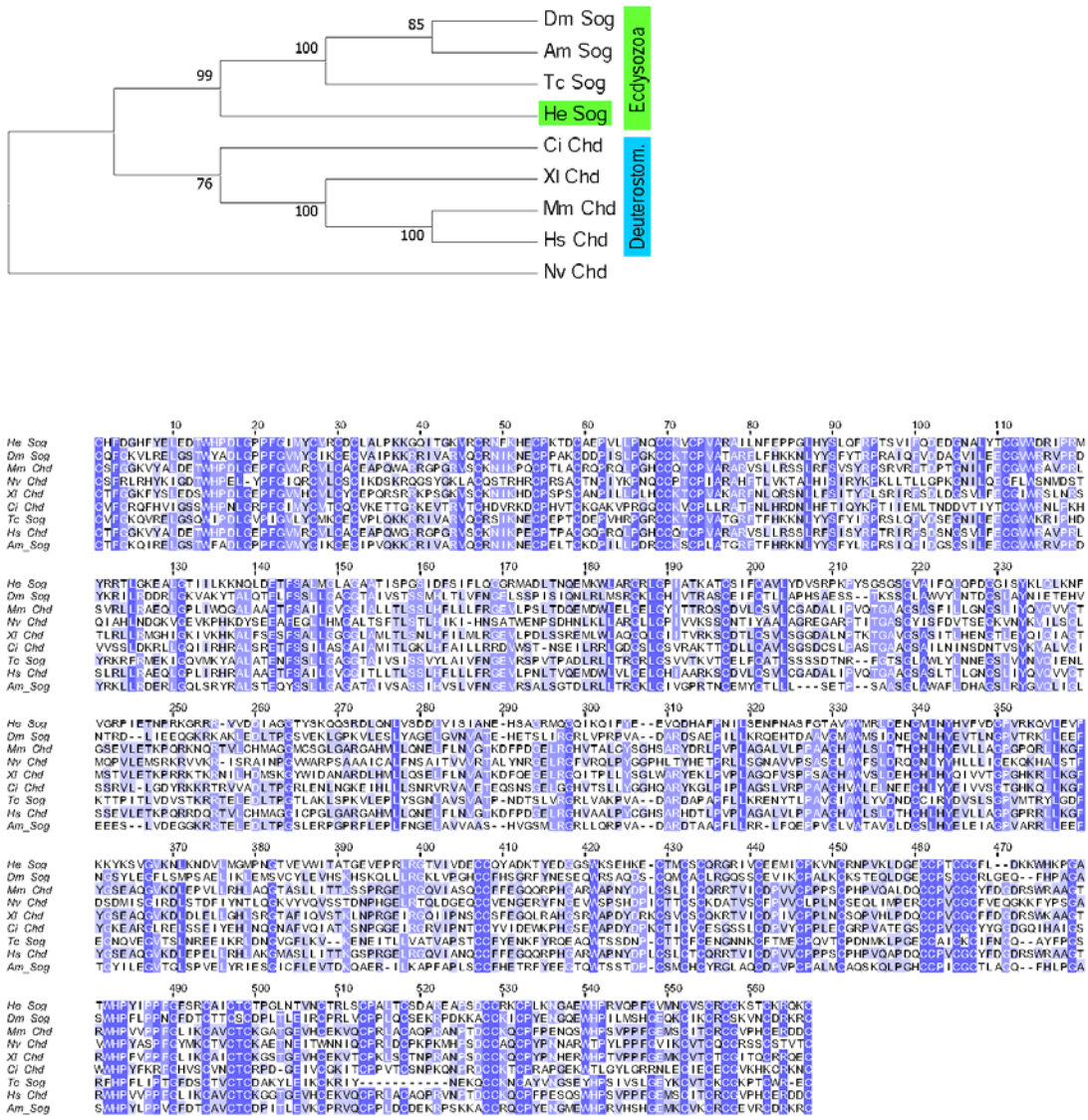

Supplementary Figure 5 Identification of a Sog homolog in *H. exemplaris*

Above: Maximum Likelihood phylogenetic reconstruction of Sog/Chordin and related amino acid sequences. Branch support out of 100 is given at each node. *H. exemplaris* sequences are highlighted. Protein families are indicated by colored bars to the right of the tree. Deuterostom = Deuterostomes. Below: Alignment used for phylogenetic reconstruction from conserved region among Sog/Chordin homologs from several species. Genes include 2-letter prefixes indicating species listed in Table 1.

Supplementary Figure 6

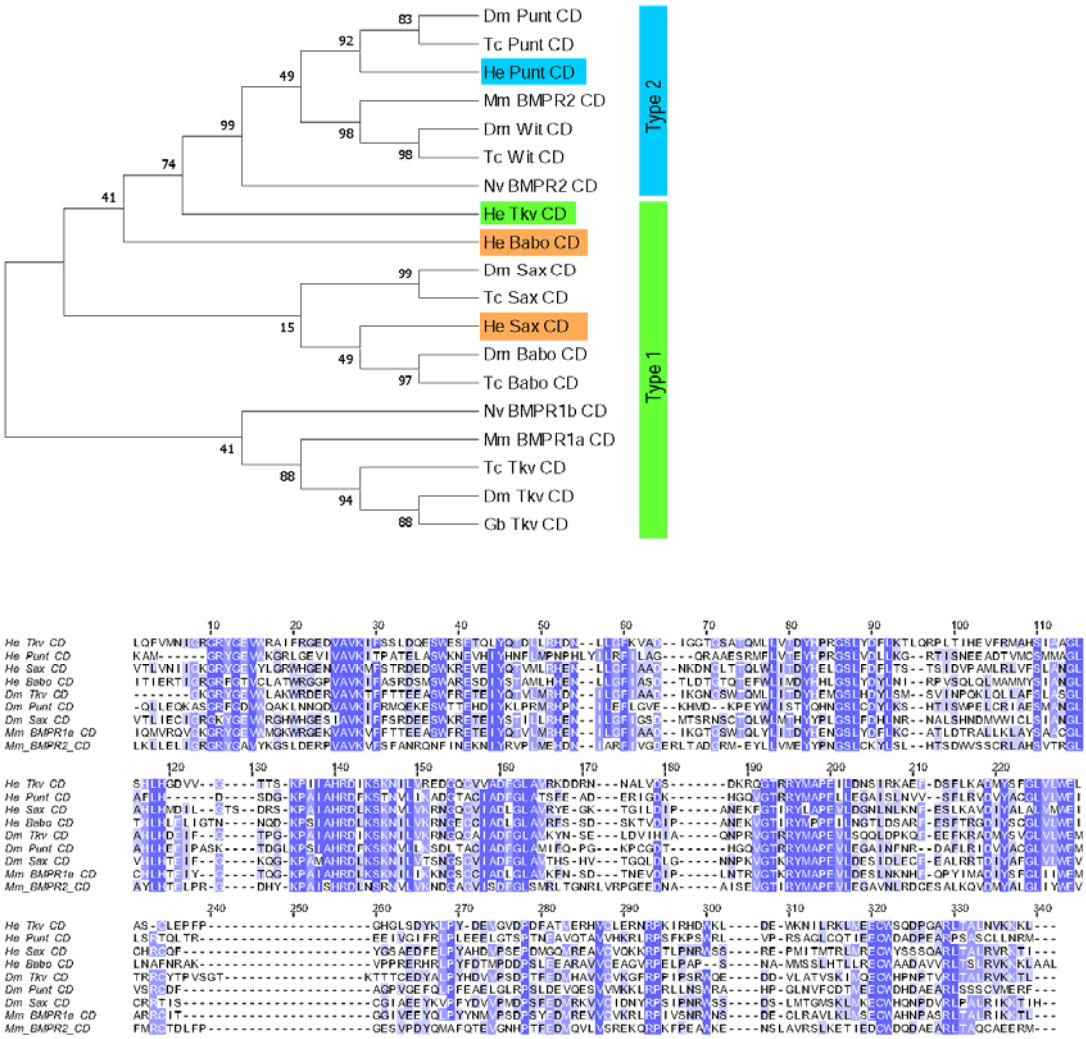

Supplementary Figure 6 Identification of BMP Type I and II Receptor homologs in *H. exemplaris*

Above: Maximum Likelihood phylogenetic reconstruction of BMP receptors Type 1 and 2 and related amino acid sequences. Branch support out of 100 is given at each node. *H. exemplaris* sequences are highlighted. Protein families are indicated by colored bars to the right of the tree. Below: Alignment used for phylogenetic reconstruction from conserved domain among BMP receptor homologs from several species. Genes include 2-letter prefixes indicating species listed in Table 1.

Supplementary Figure 7

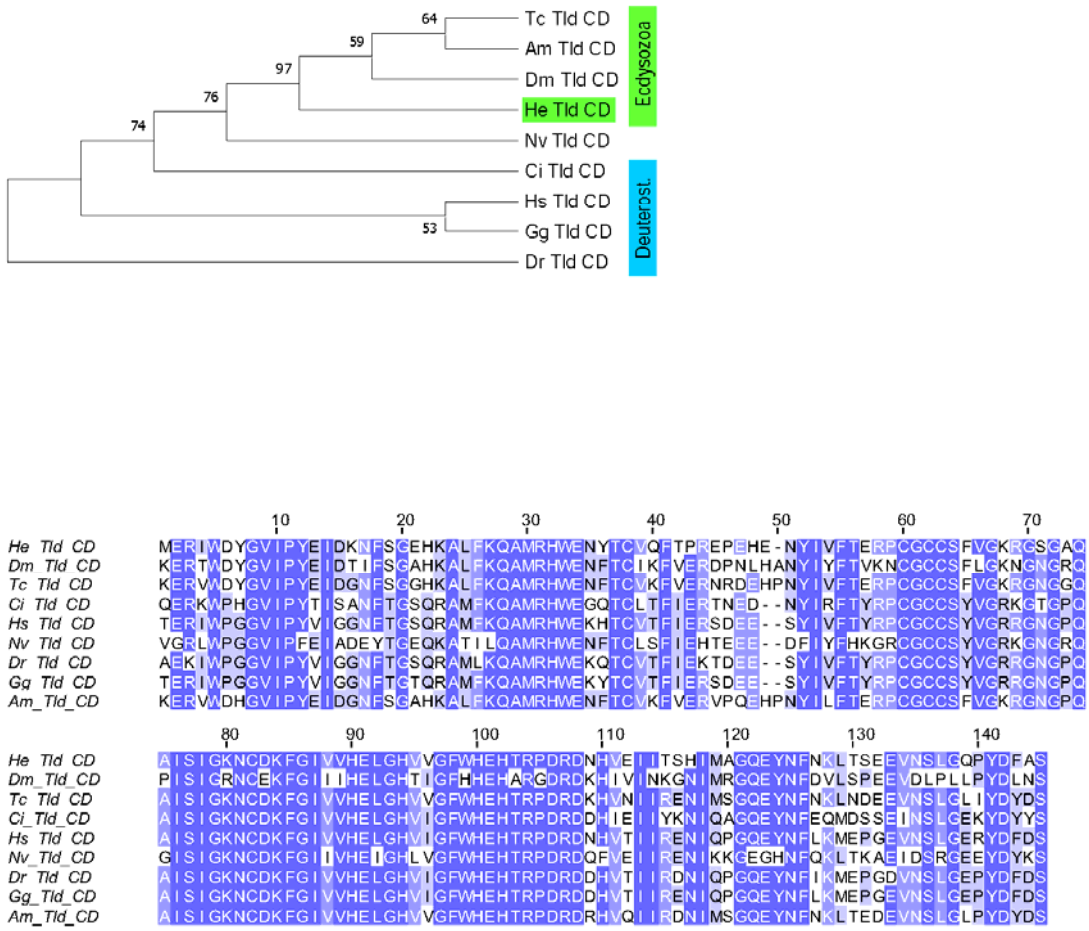

Supplementary Figure 7 Identification of a Tolloid homolog in *H. exemplaris*

Above: Maximum Likelihood phylogenetic reconstruction of Tolloid and related amino acid sequences. Branch support out of 100 is given at each node. *H. exemplaris* sequences are highlighted. Protein families are indicated by colored bars to the right of the tree. Deuterost = Deuterostomes. Below: Alignment used for phylogenetic reconstruction from conserved domain among Tolloid homologs from several species. Genes include 2-letter prefixes indicating species listed in Table 1.

Supplementary Figure 8

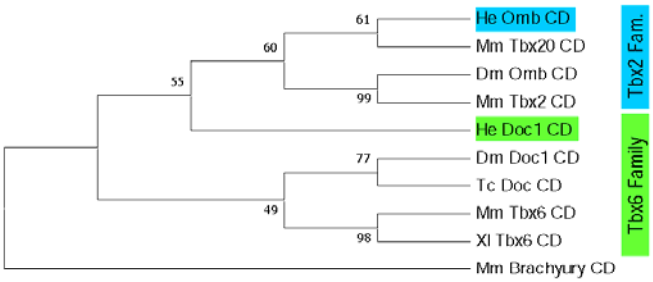

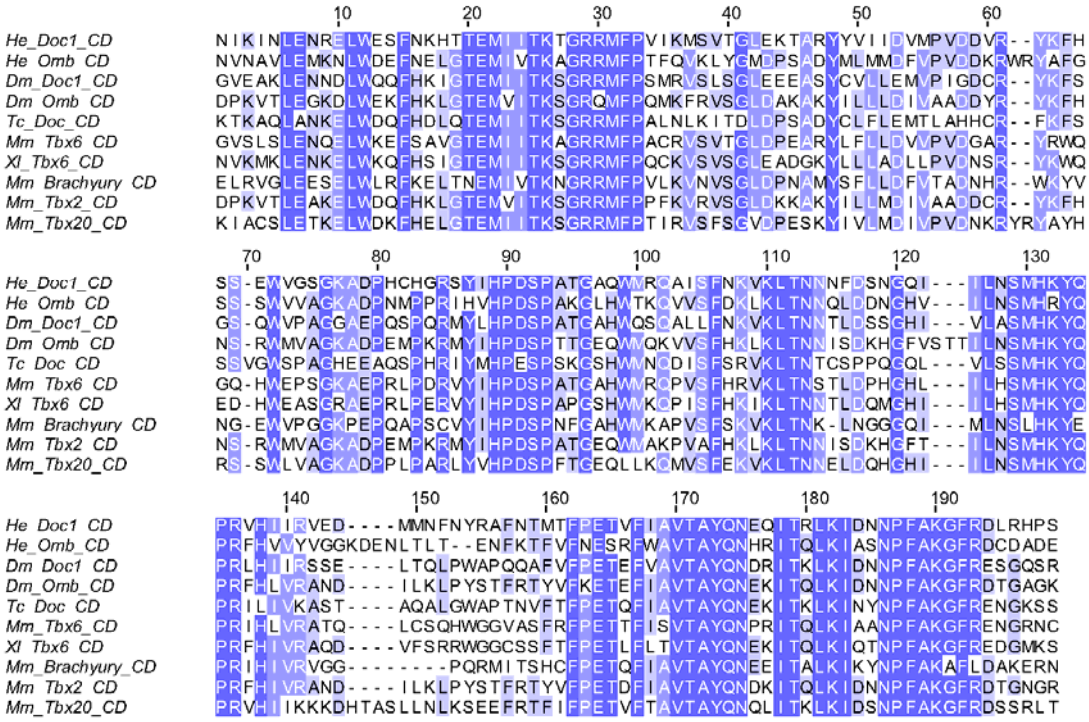

Supplementary Figure 8 Identification of a Doc1 homolog in *H. exemplaris*

Above: Maximum Likelihood phylogenetic reconstruction of Dorsocross (Doc) and Optomotor Blind (Omb) and related amino acid sequences. Branch support out of 100 is given at each node. *H. exemplaris* sequences are highlighted. Protein families are indicated by colored bars to the right of the tree. Below: Alignment used for phylogenetic reconstruction from conserved domain among Dorsocross homologs from several species. Genes include 2-letter prefixes indicating species listed in Table 1.

Supplementary Figure 9

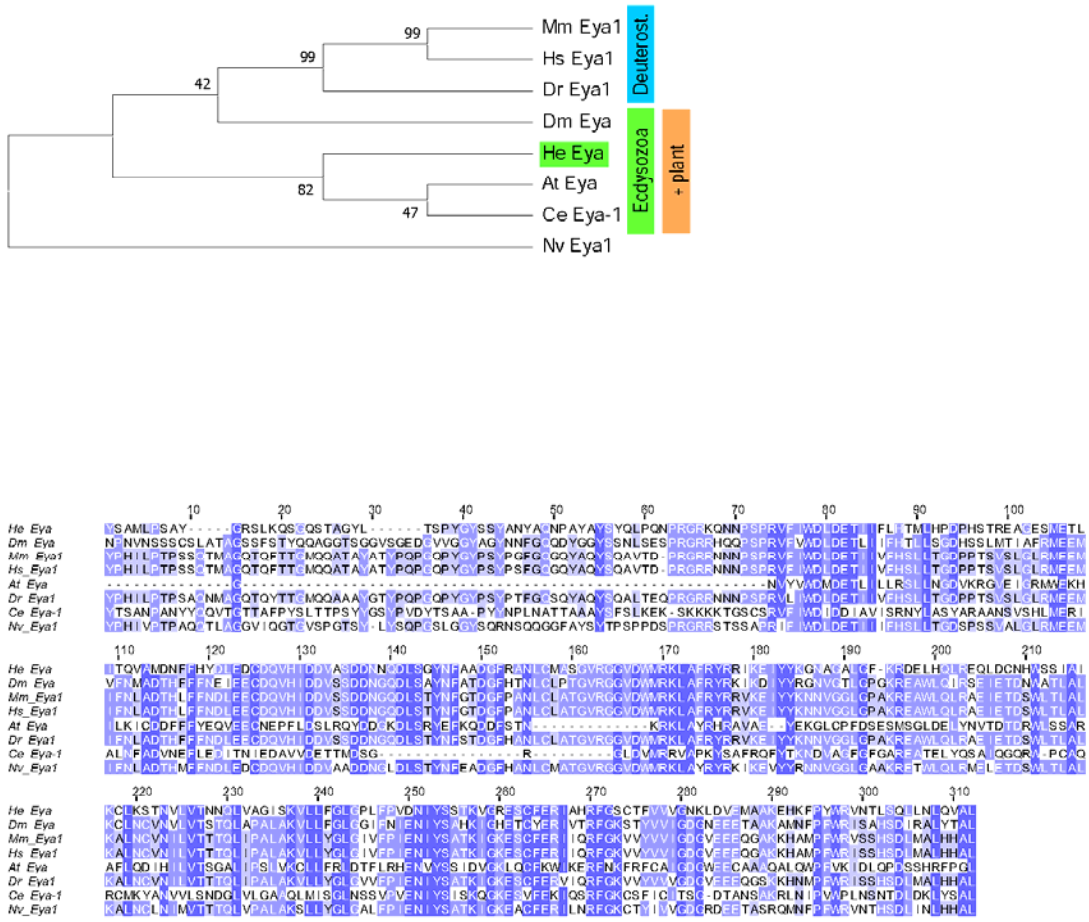

Supplementary Figure 9 Identification of an Eya homolog in *H. exemplaris*

Above: Maximum Likelihood phylogenetic reconstruction of Eyes absent (Eya) and related amino acid sequences. Branch support out of 100 is given at each node. *H. exemplaris* sequences are highlighted. Protein families are indicated by colored bars to the right of the tree. Deuterost = Deuterostomes. Below: Alignment used for phylogenetic reconstruction from conserved region among Eya homologs from several species. Genes include 2-letter prefixes indicating species listed in Table 1.

Supplementary Figure 10

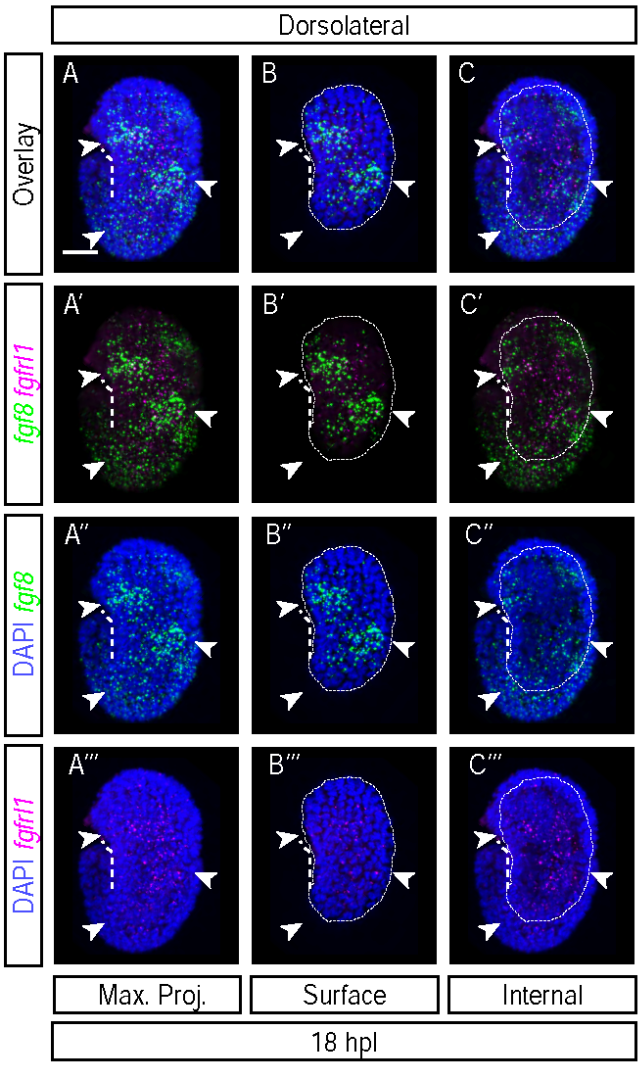

Supplementary Figure 10 Expression patterns of *fgf8* and *fgfrl1* mRNAs at elongation stage (18 hpl).

A-C. Enrichment patterns of *fgf8* and *fgfrl1* mRNAs at 18 hpl (n=2 experiments, 8 and 2 embryos). A. Maximum intensity projection of embryo from a dorsolateral view. B. Projection of uppermost layers of the embryo in A. C. Projection of internal layers of the embryo in A. Region outlined with a dashed line indicates the region with signal in the upper layers projected in B, which are omitted in the internal layers projected in C. Arrowheads indicate ectodermal patches of *fgf8* signal. Left dorsolateral view. Scale bar = 10 µm.

Supplementary Figure 11

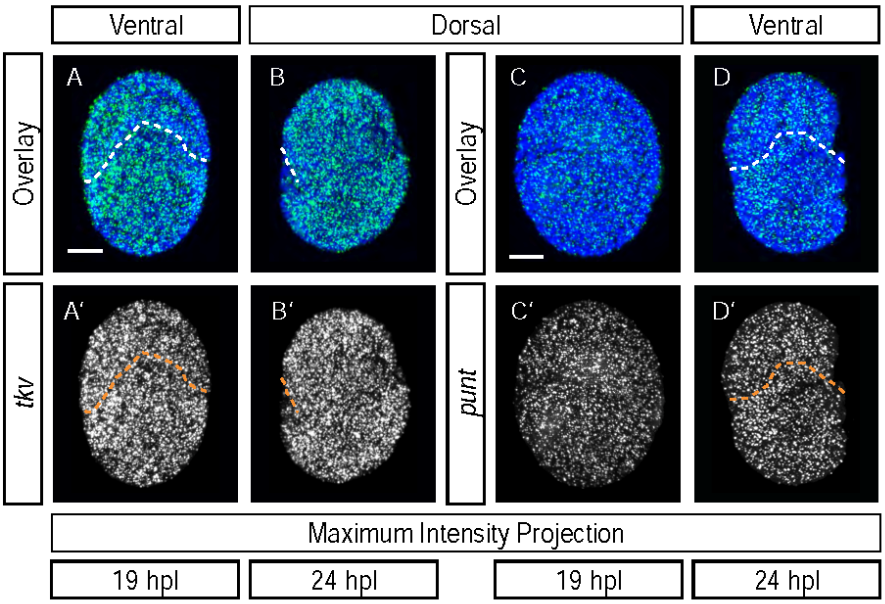

Supplementary Figure 11 Expression patterns of *tkv* and *punt* at ectodermal segmentation stage (24 hpl).

A-B. Enrichment pattern of *tkv* mRNAs at 19 hpl (A, n=1 experiment, 6 embryos) and 24 hpl (B, n=2 experiments, 7 and 4 embryos) by FISH. C-D. Enrichment pattern of *punt* mRNAs at 19 hpl (A, n=1 experiment, 4 embryos) and 24 hpl (B, n=2 experiments, 4 and 4 embryos) by FISH. All images are maximum intensity projections. Embryos are all in ventral or dorsal view, as indicated. Scale bar = 10 µm.

Supplementary Figure 12

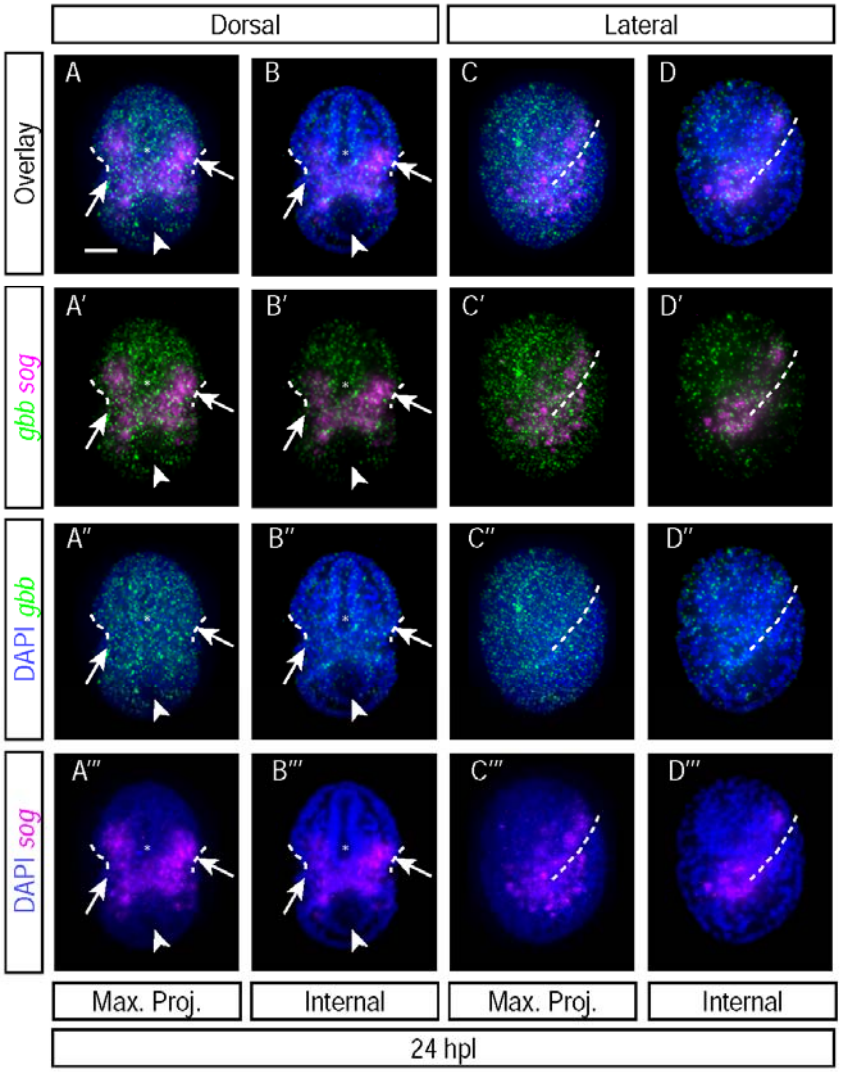

Supplementary Figure 12 Expression patterns of *gbb* and *sog* at ectodermal segmentation stage (24 hpl).

A-D. Enrichment patterns of *gbb* and *sog* mRNAs at 24 hpl (n=1 experiment, 11 embryos). A and C Maximum intensity projections of embryos from a dorsal (A) and lateral (C) view. B. Projection of internal layers of the embryo in A. D. Projection of internal layers of the embryo in C. Arrowheads in A-B indicate region of the PGCs, which is not enriched for *gbb*. Arrows in A-B indicate bands of cells enriched for *sog* on either side of the developing mouth. Asterisks in A-B indicate the hollow space within the developing foregut, which is not enriched for *sog* in its epithelium, but which does contain *gbb* signal. Dorsal view in A-B. Right lateral view in C-D. Scale bar = 10 µm.

Video Legends

Video 1 Embryo stained for *fgf8* and *fgfrl1* mRNAs at ectodermal segmentation (24 hpl) rotating about the dorsal-ventral axis.

Video curated using FIJI function: stack 3-D projection with interpolation. Annotated in Adobe Premier Pro. Arrow indicates enriched signal for *fgf8* mRNA in ectoderm. Arrowhead indicates enriched signal for *fgfrl1* mRNA in a layer more internal to the enrichment for *fgf8* mRNA. Slices are 0.364 µm in thickness. Scale bar = 10 µm.

Video 2 Embryo stained for *fgf8* and *fgfrl1* mRNAs at ectodermal segmentation (24 hpl) scrolling through z planes in 3-D.

Top right quadrant shows DAPI signal, top left quadrant shows *fgf8* mRNA signal, bottom left quadrant shows *fgfrl1* mRNA signal, and bottom right quadrant shows an overlay of all three channels. Video curated using Zen Black export function of AVI video of split channels. Annotated in Adobe Premier Pro. Slices are 0.144 µm in thickness.

Video 3 Embryo stained for *dpp* and *sog* mRNAs at ectodermal segmentation (24 hpl) rotating about the left-right axis.

Video curated using FIJI function: stack 3-D projection with interpolation. Annotated in Adobe Premier Pro. Arrow indicates absence of signal for either *dpp* or *sog* mRNA in dorsal-most ectoderm. Arrowheads indicate dorsal-most signal for *dpp* mRNA, which extends further dorsally than does *sog* mRNA. Slices are 0.397 µm in thickness.

Video 4 Embryo stained for *dpp* and *sog* mRNAs at ectodermal segmentation (24 hpl) scrolling through z planes in 3-D.

Top right quadrant shows DAPI signal, top left quadrant shows *dpp* mRNA signal, bottom left quadrant shows *sog* mRNA signal, and bottom right quadrant shows an overlay of all three channels. Video curated using Zen Black export function of AVI video of split channels. Annotated in Adobe Premier Pro. Slices are 0.397 µm in thickness.